# Synchronization of fronto-parietal beta and theta networks as a signature of visual awareness in neglect

Juliana Yordanova (1,2)*, Vasil Kolev (1,2)*, Rolf Verleger (2), Wolfgang Heide (2,3),
Michael Grumbt (4,5), Martin Schürmann (4,6)

(1) Institute of Neurobiology, Bulgarian Academy of Science, Sofia, Bulgaria
(2) Department of Neurology, Universität zu Lübeck, Lübeck, Germany
(3) Department of Neurology, Allgemeines Krankenhaus, Celle, Germany
(4) Institute of Physiology, Universität zu Lübeck, Lübeck, Germany
(5) Department of Neurology, Klinikum Bernburg, Bernburg, Germany
(6) School of Psychology, University of Nottingham, Nottingham, United Kingdom

Corresponding author:   Dr. Juliana Yordanova, Ph.D., Institute of Neurobiology, Bulgarian

Academy of Sciences, Acad. G. Bonchev str., bl. 23, 1113 Sofia, Bulgaria, tel/fax: +359-2-

979-37-49, e-mail: jyord@bio.bas.bg

Running title: Synchronization of fronto-parietal theta networks in neglect

(*) These authors contributed equally to the study

Abstract

In the neglect syndrome, the perceptual deficit for contra-lesional hemi-space is increasingly viewed as a dysfunction of fronto-parietal cortical networks, the disruption of which has been described in neuroanatomical and hemodynamic studies. Here we exploit the superior temporal resolution of electroencephalography (EEG) to study dynamic transient connectivity of fronto-parietal circuits at early stages of visual perception in neglect. As reflected by inter-regional phase synchronization in a full-field attention task, two functionally distinct fronto-parietal networks, in beta (15-25 Hz) and theta (4-8 Hz) frequency bands, were related to stimulus discrimination within the first 200 ms of visual processing. Neglect pathology was specifically associated with significant suppressions of both beta and theta networks engaging right parietal regions. These connectivity abnormalities occurred in a pattern that was distinctly different from what was observed in right-hemisphere lesion patients without neglect. Also, both beta and theta abnormalities contributed additively to visual awareness decrease, quantified in the Behavioural Inattention Test. These results provide evidence for the impairment of fast dynamic fronto-parietal interactions during early stages of visual processing in neglect pathology. Also, they reveal that different modes of fronto-parietal dysfunction contribute independently to deficits in visual awareness at the behavioural level.

*Keywords*: Neglect, Synchronization, EEG, Connectivity, theta

1. INTRODUCTION

Neglect is a common syndrome following right hemisphere damage. It is characterized by both a rightward bias in spatial sensory-motor processing and non-lateralized deficits of arousal, attentional capacity, and working memory (Husain and Rorden, 2003; Hillis, 2006; Bartolomeo et al., 2012). Traditionally, neglect has been explained in terms of localized damage of specific right-hemisphere brain structures including the inferior parietal lobe (Vallar and Perani, 1986; Mort et al., 2003), superior temporal gyrus (Karnath et al., 2004), and inferior frontal cortex (Husain and Kennard, 1996). Diverse as these sites are, lesions share core symptoms of neglect, consistent with a disconnection syndrome or failure of individual constituent nodes in frontal or parietal lobes to integrate a network-level function (Doricchi and Tomaiuolo, 2003).

Several lines of research provide support to the disconnection hypothesis. First, neuroanatomical studies of the architecture of fronto-parietal networks have shown that the dorsolateral prefrontal cortex and the posterior parietal cortex are directly and extensively interconnected in both monkeys (Petrides and Pandya, 1984; Schmahmann and Pandya, 2006) and humans via three long-distance fasciculi (Thiebaut de Schotten et al., 2011; Bartolomeo et al., 2012). Functional MRI studies have identified two major fronto-parietal networks subserving attention in humans, a bilateral dorsal one and a right-lateralized ventral one (rev. Corbetta and Shulman, 2002, 2011). Second, converging evidence exists for the role of the integrity of fronto-parietal networks in neglect pathology. It has been shown that the functional inhibition of fronto-parietal connections generates an intraoperative neglect-like pattern during a bisection line task in patients undergoing surgery (Thiebaut de Schotten et al., 2005). Using lesion-symptom mapping and fractional anisotropy, specific components of fronto-parietal fibers have been isolated that are responsible for the deficits in modulation of attention by task relevance (Ptak and Schnider, 2010) and for severity of chronic symptoms in neglect (Lunven et al., 2015). By measuring hemodynamic coherent fluctuations in the event-

related fMRI signal, He et al. (2007) were the first to demonstrate disrupted functional connectivity in fronto-parietal networks in neglect patients, as confirmed recently by analysis of resting state functional connectivity using both MRI (Baldassarre et al., 2014) and high-resolution electroencephalographic (EEG) signals (Fellrath et al., 2016).

From a functional point of view, fronto-parietal networks in healthy subjects have been associated with spatial attention and orienting, with the dorsal network related to the control of spatial and featural attention and stimulus-response mapping, and the right-lateralized ventral network linked to reorienting to unexpected but behaviorally relevant events (rev. Corbetta and Shulman, 2002). However, fronto-parietal networks also are strongly implicated with conscious processing (Dehaene and Changeux, 2011). Neuroimaging and electrophysiological studies of conscious access in humans (e.g., during attention blink, binocular rivalry, inattention blindness, etc.) have revealed that consciously accessed stimuli consistently ''ignite'' large-scale prefronto-parietal networks, in contrast to events that have remained out of consciousness (rev. Dehaene and Changeux, 2011; Driver and Vuilleumier, 2001; Rees, 2013). Transcranial magnetic stimulation (TMS) inducing transient dysfunction in parietal or prefrontal areas can prevent conscious perception and even trigger sudden subjective disappearance of visual stimuli (Kanai et al., 2008; Beck et al., 2006; Carmel et al., 2010; Babiloni et al., 2007; Kihara et al., 2011), a reduction of subjective visibility (Rounis et al., 2010), or a hemineglect-like profile (Sack, 2010). Fronto-parietal networks have also been demonstrated to subserve executive control and working memory (Egner et al., 2008; Bressler and Menon, 2010; Menon, 2013; Rottschy et al., 2012, 2013), with prominent activations found in the right hemisphere (Hardwick et al., 2013). Hence, pathologies of these networks or their long-distance connections can critically impair conscious visual perception independently of (van Boxtel et al., 2010; Sumner et al., 2006; Tsuchiya and Koch, 2008; Boehler et al., 2008) or in addition to deficits of attention and central executive networks

(Chica et al., 2013). However, the role of fronto-parietal networks for deficient conscious perception, a key symptom in neglect, has remained less well explored.

The present study aimed at evaluating the dynamic functional connectivity of fronto-parietal networks during conscious visual perception in neglect. This objective was approached by employing a task that specifically assessed the ability to integrate information from the two hemi-fields, and by applying an electrophysiological measure that specifically assesses integration between cortical areas. In our task, two squares with vertical or horizontal gratings were simultaneously presented in the left and right hemi-fields. Stimuli were non-targets when the two gratings were equal (vertical or horizontal) and were targets when the two gratings differed. The key feature of the task was that both the left and right hemi-fields were stimulated, but stimuli could be classified as targets or non-targets only by integrating information from the two hemi-fields (full-field attention task). Thus, visual awareness was challenged both in a bottom-up way, by stimulating simultaneously the two hemi-fields, and in a top-down way, by attributing task relevance to the information from the two hemi-fields (Vuilleumier et al., 2008; Ptak and Schnider, 2010; Ptak, 2012).

Our electrophysiological measures were applied to cover the temporal scales of conscious visual perception, the correlates of which emerge within 500 ms after stimulus presentation (Tononi and Koch, 2008; Roelfsema et al., 2004; Wyart and Tallon-Baudry, 2008; Dehaene and Changeux, 2011; Melloni et al., 2011; Koivisto & Grassini, 2016). Previously, disrupted functional connectivity of fronto-parietal networks in neglect has been established by analysis of MRI BOLD signals (He et al., 2007; Baldassarre et al., 2014) and resting-state EEG (Fellrath et al., 2016). However, fast dynamic coupling during perception may not be captured by the low time resolution of the fMRI and resting-state EEG signals. Instead, fast and transient network fluctuations can be reflected by the inter-regional synchronization of neuroelectric signals with high time resolution (Rodriguez et al., 1999; Fries et al., 2001; Fries, 2005; Bressler and Tognoli, 2006; Bressler and Menon, 2010).

Therefore, the spatial phase synchronization of event-related EEG oscillations was analyzed, to assess fast dynamic interactions of frontal and parietal regions. EEG was recorded in patients with right-hemisphere lesions during full-field visual task processing. Depending on the presence of neglect symptoms, patients were divided into a group with neglect and a group without neglect and were compared to age-matched healthy controls. It was expected that if dynamic fronto-parietal connectivity contributes to hemi-field perceptual deficits, the synchronization between frontal and parietal regions during visual perception would be specifically altered in patients with neglect.

## 2. MATERIALS AND METHODS

### 2.1. Participants

Three groups of participants were formed according to neurological examination directed to detect neglect symptoms by means of application of the German version of the Behavioral Inattention Test (BIT, Wilson et al., 1987). BIT consists of six paper-and-pencil tests (line bisection, line cancellation, star and letter cancellation, figure and shape copying) and nine behavioral tests (e.g. telephone dialing, reading, visual exploration of natural scenes, telling and setting the time on a clock face). The three groups were (Table 1):

(1) Patients with neglect (N+): 9 patients aged 35-78 years (median 60 years; 4 females) with right-hemisphere ischemia or hemorrhage (confirmed in CT and/or MRI, at temporo-parietal, posterior parietal, fronto-precentral, or basal ganglia locations, lesion-to-test interval 1-29 weeks, median 14 weeks) and left visual hemineglect syndrome (score below 166 in BIT, measured on-site immediately after the experiment; median 149; range 84-160). Mean lesion size was 7.6% (SD ± 1.2%, range 1.2-17.4%) of estimated brain volume, based on manual reconstruction of lesions from CT images using templates from Damasio & Damasio (1989).

6

(2) Patients without neglect (N-): 11 patients aged 50-72 years (median 60 years; 5 females) with right-hemisphere ischemia or hemorrhage. Lesions were at prefrontal, (centro-)temporal, anterior temporal, striato-lenticular, or capsular locations, sparing the classical neglect-inducing lesion sites, such as the posterior parietal lobe, the temporo-parietal junction, and in most cases also the fronto-precentral region around the frontal eye fields (confirmed in CT and/or MRI, lesion-to-test interval 5 weeks to 4.5 years, median 13 weeks). In these patients there was no hemineglect syndrome at the time of investigation (BIT score: median 169; range 167.5-170) and no history of a past hemineglect syndrome. Mean lesion size was 2.2% (SD ± 1.9%, range 0.3-6.3%), being significantly smaller than in N+ patients ($F(1/19) = 6.7$, $p = 0.02$). However, lesion size did not correlate with BIT scores across all patients (Pearson correlation coefficient, $r = -0.08$, $p > 0.7$) nor separately in either the N- ($p > 0.7$) or the N+ group ($p > 0.2$).

(3) Control group: 14 persons aged 52-76 years (median 60.5 years; 8 females) without any history of neurological disorders.

Four other N+ patients and four other control subjects had participated but had to be excluded from data analysis because of insufficient number of artefact-free trials for EEG analysis.

In all participants, visual acuity was measured immediately before the experiment and found to be better than 0.7. All subjects who took part in the study gave informed written consent according to the Declaration of Helsinki. The experiment was approved by the local ethics committee.


2.2. Task and procedure

Subjects were seated comfortably in a chair in a dimly illuminated sound-protected room. As illustrated in Fig. 1, two types of visual stimuli were presented – horizontally and vertically oriented sinusoidal gratings with a spatial frequency of 1.3 cycles per degree of visual angle

(c/deg) and mean luminance of 80 cd/m$^2$. Stimuli were presented on a 17" CRT display, and were viewed from 1.5 m distance, resulting in a stimulus size of 12 x 9 degrees. Stimulus content depended on the integration of information from the two visual fields, left and right. Non-targets were stimuli with identical left and right visual fields (either both with horizontal or both with vertical grids). Targets were defined as having different right and left visual fields (i.e., horizontal in one field and vertical in the other). Targets and non-targets were presented in random order, with probabilities of 33% for targets and 67% for non-targets.

Each trial started with a blank gray screen (1024 ms) then the stimulus was displayed for 67 ms, followed by 700 ms of blank gray screen. Immediately afterwards a question mark was displayed in the center of the screen. A response-button was fixed on the right armrest of the chair such that it could be comfortably pressed with the right index finger. Participants were instructed to produce a delayed response to targets by pressing the response-button once the question mark had appeared. Inter-trial intervals (from onset of one stimulus to the next) varied randomly between 4.1 and 4.6 s. A central fixation dot was present throughout the experiment, superimposed on blank screens, stimuli, and question mark.

## 2.3. EEG recording

EEG was recorded with Ag/AgCl electrodes from 13 scalp sites according to the International 10/20 system (F7, F3, F4, F8, C3, Cz, C4, P7, P3, P4, P8, O1, and O2) against linked mastoids as a reference, with a ground electrode positioned on the forehead. Horizontal and vertical electrooculograms (EOG) were also recorded. EEG was amplified with band limits of 0.1 and 70 Hz (additional 50 Hz notch filter, -24db/octave), digitized at 500 Hz and stored on a PC-based EEG acquisition system (Brain Data, Lübeck, Germany).

## 2.4. Data analysis
### 2.4.1. Performance analysis

Target identification required button pressing. Missing responses to targets were considered as omission errors (OE). Motor responses to non-targets were considered as commission errors (CE). Error rate measures were subjected to a 3-way repeated measure analysis of variance (ANOVA) with the between-subjects factor Group (controls vs. N- vs. N+) and within-subjects factors Stimulus (target vs. non-target) and Left-Side Grating (vertical vs. horizontal). Reaction times were averaged across trials with correct responses and submitted to the same ANOVA.

2.4.2. EEG data analysis

Pre-processing was performed by Brain-Vision Analyzer 2.0.3 software and included splitting the data into appropriate segments for analysis, editing for artifacts, and EOG correction according to Gratton et al. (1983). An epoch of 2048 ms was used for analysis, with 1024 ms before and 1024 ms after stimulus. Segments with amplitudes exceeding ±125 µV at any EEG electrode were discarded and the remaining segments were visually checked for artifacts. To increase signal/noise ratio, trials were pooled across grating directions (vertical and horizontal). Thus, the mean number of artifact-free correct trials in the three groups N+, N-, and controls was 53, 63, 66 for targets and 109, 132, 131 for non-targets. Minimum values were 38, 44, 64 for targets and 57, 127, 109 for non-targets. Due to insufficient number of artifact-free error trials in half of the patients with neglect, only correct trials were analyzed. Analyses of event-related EEG activity in both time and time-frequency domains were performed against a pre-stimulus baseline of 250 ms before stimulus.

2.4.3. Time-domain analysis

For analysis of visual event-related potentials (ERPs) in the time domain individual single sweeps of correct responses were averaged for each group, electrode and stimulus type. The visual P1 component was identified as the most positive peak within 120 ms after stimulus

N1 (the most negative component within 100-200 ms after stimulus onset) was composed of two sub-components, an early one within 110-140 ms and a late one within 140-180. Accordingly, N1 was measured as the mean amplitude of the potential in these two latency windows.

2.4.4. Time-frequency decomposition

Time-frequency (TF) analysis of ERPs was performed by means of a continuous wavelet transform (CWT, Mallat, 1999) with Morlet wavelets as basis functions. Complex Morlet wavelets $W$ can be generated in the time domain for different frequencies, $f$, according to the equation:

$$W(t, f) = A \exp(-t^2 / 2\sigma t^2) \exp(2i\pi f t),$$

where $t$ is time, $A = \left(\sigma_t \sqrt{\pi}\right)^{-1/2}$, $\sigma_t$ is the wavelet duration, and $i = \sqrt{-1}$. TF decomposition was performed on single trials. In order to optimize frequency and time resolution, CWT parameters were chosen to target specifically slow and fast frequencies.

A. Analysis of low-frequency TF components. For this analysis, the wavelet family was characterized by a ratio of $f_0/\sigma_f = 4$, where $f_0$ is the central frequency and $\sigma_f$ is the width of the Gaussian shape in the frequency domain. The choice of the ratio $f_0/\sigma_f$ was oriented to the expected slower components. The analysis was performed in the frequency range 0.5–16 Hz with central frequencies at 0.4 Hz intervals. For different $f_0$, time and frequency resolutions can be calculated as $2\sigma_t$ and $2\sigma_f$, respectively. $\sigma_t$ and $\sigma_f$ are related by the equation $\sigma_t = 1/(2\pi\sigma_f)$.

B. Analysis of high-frequency TF components. The wavelet family was characterized by a ratio of $f_0/\sigma_f = 12$. The choice of the ratio $f_0/\sigma_f$ was oriented to fast-frequency

components to provide for optimal time/frequency resolution. The analysis was performed in the frequency range 15–50 Hz (beta-gamma) with central frequencies at 0.875 Hz intervals.

According to the results (Fig. 2), one relevant TF component was measured with central frequency $f_0 = 5.5$ Hz ($2\sigma_t = 232$ ms, and $2\sigma_f = 2.75$ Hz), and another one with central frequency $f_0 = 22$ Hz ($2\sigma_t = 173$ ms, and $2\sigma_f = 3.67$ Hz).

### 2.4.5. Spatial phase-locking or between-sweep-between-electrode synchronization

Following methodological recommendations (Cohen, 2015), phase-based connectivity was assessed using phase-locking values (PLVs). This approach (a) is recommended for hypothesis-driven analysis as targeted here, rather than for exploratory analyses; (b) is robust to time dynamics, time lag, frequency mismatches, and frequency non-stationarities, as expected for event-related EEG responses; and (c) is robust to increased variance in phase stability, as expected for pathology.

PLVs between electrode channels measure the extent to which oscillation phase angle differences between electrodes are consistent over trials at each time/frequency point (e.g., Varela et al., 2001). As a measure of spatial synchronization, PLVs were computed for different TF scales at each time-point $t$ and trial $j$ according to the equation:

$$PLV_{k,l} = \left| \frac{1}{N} \sum e^{i\left(\left(\rho_{j,k}(t,f_0) - \rho_{j,i}(t,f_0)\right)\right)} \right|,$$

where $N$ is the number of single sweeps, $k$ and $l$ are indices for the pair of electrodes to be compared, and $\rho$ is the instantaneous phase of the signal. $PLV_{k,l}$ results in real values between one (constant phase difference) and zero (random phase difference). First, time-frequency plots of PLV for all electrode pairs (78 pairs from 13 electrodes) pooled together were computed to identify relevant frequency bands supporting global connectivity and their timing. Time-frequency plots of PLV for targeted fronto-parietal pairs were also computed. Accordingly, PLV measurements were performed for each participant for all electrode

combinations pooled together (global synchronization) and for each fronto-parietal electrode combination. Basing on observations of PLV TF plots (Figure 2A,B) mean values and peak latencies of the CWT layers corresponding to beta ($f_0$ = 22 Hz for the time window 0-250 ms) and theta range ($f_0$ = 5.5 Hz for the time window 0-300 ms) were measured. Before statistical evaluation, mean values were normalized by subtracting the mean value of a baseline (pre-stimulus) period of 250 ms.

2.4.6. Control analysis measures

PLV is not protected against volume conduction or against simultaneous independent activations at multiple regions during external stimulation. This is in contrast to the phase-lag index (PLI), another quantifier of phase-based connectivity (Stam et al., 2007), which reflects consistency of inter-regional phase relationships, but may be less sensitive to time dynamics, frequency non-stationarity, and increased variance, due to the elimination of simultaneous phase-coupling from the final estimate. Therefore, to increase confidence in PLV results, (1) PLI also was computed and used for control analyses, and additional follow-up control tests using the power and local (inter-trial) phase locking of ERPs were performed. Other control analysis measures were: (2) Total Power of time-frequency components, to perform post-hoc tests controlling for volume conduction and common-source effects (Cohen, 2015); (3) Phase-locking factor (PLF), to assess the local phase-locking (inter-trial synchronization) of time-frequency ERP components (Lachaux et al., 1999; Tallon- Baudry et al., 1997) and control for the contribution of independent stimulus-induced synchronizations at multiple regions to PLV. Following the PLV observations (Results, 3.3), all control analyses were performed for the relevant frequency ranges, beta and theta. Methodological details on the computation and analysis of these parameters are presented in Suppl. 4.

2.4.7. Statistical evaluation

Repeated-measures ANOVA was applied to PLV measures. Fronto-parietal (FP) PLVs were analyzed in one global ANOVA for the 16 F-P electrode pairs from each of the four frontal (F7, F3, F4, and F8) with each of the four parietal (P7, P3, P4, P8) sites. Factors were laterality of the frontal member of these F-P pairs (Lat-F), left (F7, F3) vs. right (F8, F4), laterality of the parietal member of these F-P pairs (Lat-P), left (P7, P3) vs. right (P8, P4), position of the frontal member according to the dorsal (F3, F4) vs. ventral (F7, F8) dimension (DV-F), and position of the parietal member according to dorsal (P3, P4) vs. ventral (P7, P8) dimension (DV-P). Thus, in the overall repeated measures ANOVA design, the within-subjects variables were Stimulus (target vs. non-target), Lat-F, Lat-P, DV-F, and DV-P, and the between-subjects variable was Group with three levels (control vs. N- vs. N+). This statistical design was expected to reveal if alterations of F-P synchronization in pathology would be determined by deficits between specific fronto-parietal systems in the right or in the left hemisphere, or by region-specific dysfunctions that would affect the functional connectivity of that particular region with all other regions. When significant interactions were obtained, simple effects of within-subjects variables were tested as described in Results, and simple groups effects were explored using MANOVA. Multiple step-wise regression analyses were performed and Pearson correlation coefficients were computed to assess the associations between PLV measures and patients' BIT scores, performance, and lesion-to-test intervals, as well as the associations between PLV and other inter-regional and local synchronization measures (control analyses). To assess the between-group differences in the synchronization of different classes of inter-regional connections, $\chi^2$ statistics were applied as specified in the results. The statistical outcome was corrected for multiple tests by means of the Bonferroni procedure.

## 3. RESULTS

### 3.1. Performance

By definition, BIT scores were pathologically decreased in neglect (N+) patients (mean 138, SE ± 8.3) and were lower than in the N- group (mean 169, SE ± 0.3; $F_{(1/18)} = 14.1$, $p < 0.001$). Reaction times did not differ among groups ($p > 0.9$), as expected from the delayed response instruction. However, error rates were substantially higher in neglect patients (commission 33.3 %, SE ± 9.9, omission 22.1%, SE ± 5.2) in comparison with both controls (commission 2.2 %, SE ± 1.8, omission 2.4%, SE ± 1.7; $F_{(1/21)} = 11.4$, $p < 0.005$) and with the N- group (commission 3.8 %, SE ± 2.9, omission 6.9%, SE ± 3.7; $F_{(1/18)} = 6.8$, $p < 0.05$). Since about 29% of responses in neglect patients were incorrect ($33\% \times 2/3 + 22\% \times 1/3$), some of these patients did not perform far from chance level. Nevertheless, only correct responses were included in the EEG analysis. No difference in error rate existed between control and N- groups ($p > 0.4$).

3.2. Visual event-related potentials

Visual ERPs were analyzed at occipital and parietal regions to reflect the local functional engagement of these areas (Di Russo et al., 1998) during relevant fronto-parietal synchronizations studied here (Suppl. 3). Supplementary Figure 2 demonstrates P1 (mean latency 92 ms, SE ± 2 ms) and N1 components (mean latency 156 ms, SE ± 3.2 ms), with N1 manifesting early (110-140 ms) and late (140-180 ms) sub-components. Only the late N1 sub-component was reduced in neglect patients, being almost absent at right dorsal parietal and occipital electrodes (Laterality x Electrode x Group, $F_{(4/60)} = 3.2$, $p = 0.03$; Simple Group effects at O2, $F_{(2/32)} > 4.2$, $p < 0.05$). P1 peak latency and amplitude did not depend significantly on pathology (Suppl. 3).

3.3. Time-frequency characteristics of fronto-parietal oscillatory networks

Time-frequency PLV plots presented in Fig. 2A demonstrate that fronto-parietal connectivity was supported by synchronizations in two frequency ranges. One dominating TF component

was in the beta (15-25 Hz) range. As shown in Fig. 2B, it was expressed within 200 ms after stimulus onset, being maximal at around 120 ms (mean 124 ms, SE ± 5.4). The second prominent TF component was in the theta (4-8 Hz) range appearing within 400 ms after stimulus onset with maximal expression at 160 ms (SE ± 7.5). Beta and theta TF components were observed in all groups. A fast-frequency component in the gamma range (30-35 Hz) also was detected in controls (Suppl. Fig. 1A) but was not further analyzed as not being pronounced above the noise level in patient groups.

Figure 2B illustrates that the temporal dynamics of inter-regional beta and theta synchronizations was similar across pairs. Fronto-parietal PLV peak latency did not depend on group ($F(2/31) < 1.8$, $p > 0.3$) despite longer beta latencies in N+ patients (mean 134 ± 8.6 ms). Figure 2B further indicates that in neglect patients, theta synchronization manifested a clustering of distribution across pairs implying a specific mode of fronto-parietal functioning, whereas fronto-parietal beta PLV was decreased in a more diffuse manner.

3.4. Specificity of fronto-parietal oscillatory networks

Time-frequency specificity: To explore if the synchronization between frontal and parietal regions was frequency-specific, global PLV was computed for all 78 channel combinations pooled together. Grand average TF plots of global PLV (Suppl. Fig. 1B) reveal the same dominant TF components as found for FP synchronization, indicating that beta and theta networks supported distributed inter-regional connectivity in this task.

Regional specificity: To explore if the synchronization between frontal and parietal regions represents a specific source of variation in patients, all 78 electrode pairs were grouped into 10 classes according to anatomical cortical regions illustrated in Fig. 3: fronto-frontal (FF), fronto-central (FC), fronto-parietal (FP), fronto-occipital (FO), centro-central (CC), centro-parietal (CP), centro-occipital (CO), parieto-parietal (PP), parieto-occipital (PO), and occipito-occipital (OO). For each class, the distribution of target and non-target PLV

measures from all groups was computed and each subject's values were classified according to being above or below the PLV median of the respective class. Using $\chi^2$ statistics, the numbers of classified cases in each group were compared. The statistical outcome was corrected for multiple tests by means of the Bonferroni procedure.

Figure 3 shows that a statistically significant distinction of the N+ group was yielded for FC, FP and FO pairs in the beta range. For these classes, N+ patients differed significantly from both healthy controls ($\chi^2$ (1/736) > 13.1, p < 0.0003) and patients without neglect ($\chi^2$ (1/640) > 9.0, p < 0.003). In contrast, significant group effects for CP beta connectivity stemmed from pathological enhancement of PLV in N- patients. Notably, beta synchronization was substantially enhanced for the majority of pairs engaging frontal and central regions in patients without neglect.

In the theta range, a significant reduction in neglect patients was observed only for FP pairs ($\chi^2$ (2/1088) = 14.3, p = 0.008). The reduction of FC theta PLV was not specific for the N+ group (N- vs. N+, $\chi^2$ (1/480) = 0.001, p = 1). Inter-hemispheric theta synchronization between homologous occipital and parietal regions tended to be enhanced in the two patient groups (Fig. 3B). These observations demonstrate that the beta network affected by pathology is broadly distributed at frontal, parietal, occipital, and central regions, being over-synchronized in N- but substantially desynchronized in N+ patients. Also, they identify the synchronization of FP theta networks as specifically impaired in patients with neglect.

3.5. Pathology-related and functional characteristics of fronto-parietal networks

Beta

Figure 4A presents grand average inter-electrode plots of beta PLV for all fronto-parietal pair combinations in the three groups of participants. Although the main group effect on FP beta PLV was not significant (Group, (F(2/31) = 1.9, p = 0.17), N+ patients manifested a significant PLV suppression for pairs grouped by right parietal regions P4 and P8 (Lat-P x

Group (F(2/31) = 4.7, p = 0.015). As illustrated in Fig. 4B and verified by post-hoc MANOVA, PLV of pairs originating from P4 and P8 electrodes was suppressed in N+ patients as compared to both controls (F(1/21) = 5.3 – 6.2, p = 0.02 – 0.03) and patients without neglect (F(1/18) = 4.8-18.1, p = 0.04 - 0.0001). Accordingly, only in the N+ group, was there a significant suppression of beta connectivity at right as compared to left parietal regions (Lat-P, F(1/8) = 14.7, p = 0.005) for both targets and non-targets (Fig. 4). A complex interaction Lat-F x DV-F x Lat-P x DV-P x Group, F(2/31) = 5.5, p < 0.01 reflected a most prominent reduction in neglect patients for right parietal/left frontal PLV (Fig. 4B), as well as the observation that beta PLV for these pairs was higher in the N- group as compared not only to patients with neglect but also to healthy controls.

Figure 4A further demonstrates that targets were associated with a significant suppression of beta PLV as compared to non-targets (Stimulus, (1/31) = 5.1, p = 0.03), but this was only valid in controls (Stimulus x Lat-P x DV-P x Group, (F(2/31) = 3.6, p = 0.04; Stimulus effect in controls, F(1/13) = 11.0, p = 0.006). This target-related suppression was most pronounced for right parietal regions (Stimulus x Lat-P in controls, (F(1/13) = 7.2, p = 0.02), especially those linked to left frontal area F3 (p<0.002 for each comparison; Stimulus x Lat-P x DV-F x Lat-F (F(1/13) = 5.3, p = 0.02). The Stimulus effect was not significant in patient groups.

Theta

The overall level of fronto-parietal theta synchronization was not affected by pathology (Group, F(2/31) = 1.0, p = 0.4), but the organization of networks was deviant, as indexed by significant interactions with Lat and DV factors.

First, Fig. 5A shows that in contrast to beta, the theta network was basically organized in a region-specific manner, i.e., synchronizations guided by one region were similar. Also, a ventral-dorsal distinction was evident. Specifically, the regional parietal synchronization was

dominated by ventral parietal regions at P7 and P8, and PLV was reduced for pairs focused at dorsal parietal electrodes P3 and P4 (DV-P, $F(1/31) = 21.6$, $p < 0.0001$). These effects were pathologically enhanced in patients (Fig. 5A) depending on stimulus processing as detailed below. Further, the regional frontal synchronization guided by dorsal frontal electrodes F3 and F4 was stronger as compared to ventral frontal electrodes F7 and F8 in controls, in contrast to patients (DV-F x Group, $F(2/31) = 5.8$, $p = 0.007$; Suppl. 2).

Second, regional parietal synchronization in control and patient groups depended on stimulus processing. This was reflected by complex interactions Stimulus x Lat-P x Group, $F(2/31) = 3.8$, $p = 0.05$; Stimulus x DV-P x Group, $F(2/31) = 6.0$, $p = 0.005$; Stimulus x Lat-P x DV-P x Group, $F(2/31) = 3.9$, $p = 0.03$. In controls, the stimulus effect was not significant ($p > 0.2$). In patients without neglect, PLV to both targets and non-targets was reduced for pairs grouped by the left dorsal parietal region P3, whereas it was enhanced for right ventral parietal pairs at P8 (DV-P, $F(1/10) = 6.8$, $p = 0.03$; DV-F x DV-P x Lat-P, $F(1/10) = 6.2$, $p = 0.03$) (Fig. 5A). In N+ patients, there was a significant stimulus effect (Stimulus, $F(1/8) = 6.5$, $p = 0.03$) due to an overall reduction of PLV for non-targets and a prominent enhancement for pairs grouped by P7 for targets (Stimulus x DV-P, $F(1/8) = 6.6$, $p = 0.03$; Stimulus x Lat-P, $F(1/8) = 9.1$, $p = 0.02$) (Fig. 5A and Suppl. 2).

The complex interaction Stimulus x Lat-F x DV-F x Lat-P x DV-P x Group ($F(2/31) = 3.4$, $p = 0.05$) further pointed to stimulus-dependent group differences at specific pairs not grouped by regions. Repeated-measures ANOVA was used to test Group x Stimulus effects at individual pairs, and MANOVA was used to test group effects at each pair in each stimulus condition. As demonstrated in Fig. 5B, groups differed significantly at F3-P3 ($F(2/31) = 3.9$, $p = 0.05$), due to PLV reduction in both N- ($p = 0.03$) and N+ ($p = 0.05$) patients relative to controls, and F4-P4 due to a significant PLV reduction in neglect patients ($F(2/31) = 3.8$, $p = 0.05$; Controls vs. N+, $p = 0.05$). Control vs. N- difference at F3-P3 was significant for both targets and non-targets ($p < 0.05$). Control vs. N+ difference at F3-P3 and F4-P4 also was

significant for both targets and non-targets (p < 0.05). Group effects for pairs at ventral P7 and P8 electrodes were significant only for non-targets due to lower values in neglect (Stimulus x Group, $F_{(2/31)} = 5.3 – 7.8$, $p = 0.01 – 0.002$). Contrasting N+ and N- patients yielded significant differences for right-hemisphere pairs F4-P8 and F8-P8 ($F_{(1/32)} = 4.1 – 4.6$, $p = 0.05$).

## 3.6. Regression analyses

BIT scores correlated strongly with the rate of commission errors (incorrect responses to non-targets, $r = -0.8$, $p < 0.001$, $n = 20$, N- and N+) and with the rate of omission errors (erroneous missing responses to targets, $r = -0.46$, $p = 0.02$, $n = 20$). A multiple stepwise regression analysis was conducted, in which the dependent variable was the BIT score and the independent predictors were beta and theta PLV values from fronto-parietal pairs to target and non-target stimuli. The model ($R=0.739$, $F_{(1/19)} = 10.22$, $p = 0.001$) extracted two independent predictors of BIT: (1) beta PLV of the right parietal/left frontal pair P4F7 to non-targets ($B =80.58$, Beta $= 0.52$, $p = 0.007$), and (2) theta PLV of the right dorsal pair P4F4 to targets ($B = 35.4$, Beta $= 0.43$, $p = 0.02$). To control if the selection of the beta predictor was due to pathological enhancement of beta synchronization in N- patients, analysis was redone only with N+ patients. Beta PLV of the right parietal/left frontal pair P4F7 to non-targets was selected also in the N+ only analysis ($R=0.631$, $F_{(1/8)} = 6.6$, $p = 0.03$, $B =101.2$, Beta $= 0.63$, $p = 0.03$). Commission error rate also was strongly predicted by beta PLV of right parietal/left frontal pair P4F3 ($R=0.746$, $F_{(1/19)} = 22.6$, $p < 0.001$, $B = -158.5$, Beta $= -0.75$, $p < 0.001$). No reliable association was found between the lesion-to-test interval and PLV.

## 3.7. Control Analyses

Only main results of control analyses are given here. A detailed description of control analyses is presented in Suppl. 4.

### 3.7.1. Phase-lag index (PLI)

PLI values were analyzed with the ANOVA design used for PLV to check for the presence of major effects. Beta PLI analysis only partially confirmed PLV findings. Beta PLI was reduced in the N+ group for pairs including right frontal electrodes and the right parietal electrode P8. The specific right parietal-left frontal phase relationship in N+ patients was not confirmed, but the enhancement of synchronization between these regions was confirmed for N- patients. In contrast to beta, theta PLI analysis basically confirmed major PLV results.

### 3.7.2. Inter-trial synchronization (PLF)

To control for the contribution of local regional synchronization to PLV, regional distribution of PLF was evaluated and compared between groups. PLF results demonstrated that local stimulus-related beta synchronization was not affected by pathology, whereas local theta synchronization was substantially reduced at all parietal electrodes in the two patient groups, with no difference between patients without and with neglect. These effects do not support the assumption that stimulus-induced synchronization at multiple regions may determine PLV estimates in patient groups.

### 3.7.3. The effect of local synchronization on PLV

To further evaluate the possible effects of independent stimulus-induced synchronization at multiple regions on PLV, first we tested if PLVs grouped by single electrodes would differ. If PLV were essentially determined by local stimulus-related synchronizations, no difference would exist between pairs that include the same electrode. For each electrode, significant theta PLV differences existed for 50-100% of the comparisons ($p = 0.001$-$0.05$, Bonferroni corrected $p < 0.005$ for more than 50% of the comparisons), irrespective of whether the local synchronization was large or weak. Beta PLV differences also were present although only as a trend in 10-30% of the pairs ($p = 0.02 – 0.05$). These observations demonstrate that local stimulus-induced synchronization might not be a critical determinant of PLV.

In a second analysis including participants from all groups, the correlations between PLV, PLI, PLF and total power were explored. PLVs that included any given electrode were averaged to reflect synchronization guided by that specific electrode. Similarly, PLIs guided by each specific electrode were averaged. Multiple step-wise regression analyses were performed for each electrode where PLV was the dependent variable, and PLI, PLF and total power at that electrode were the predictors. For all analyses of theta PLV, theta PLI was selected as a significant predictor ($p < 0.001$). PLI prediction was weaker for beta PLV as PLI was selected as an independent predictor of PLV in half of the models at parietal electrodes. These control observations indicate that PLV measures are basically predicted by PLI measures, which are free of volume conduction and stimulus-induced phase-locking effects, and therefore appear to reflect essential inter-regional connectivity.

### 3.7.4. Correlations between power measures.

To further exclude volume conduction effects on PLV, correlations between total power measures at frontal and parietal electrodes were tested. In case of inter-regional synchronizations induced by a common source or volume conduction, strong positive correlations are expected between the power measures at frontal and parietal electrodes (Cohen, 2014, 2015). Most of these correlations were negative ($r = - 0.2/ -0.004$) and those that were positive did not reach significance. These post-hoc tests provide additional arguments for PLV measures used here not being produced by common sources.

### 3.7.5. PLV of equidistant pairs.

Additional support comes from comparisons of our intra-hemispheric PLVs with PLV of equidistant trans-hemispheric pairs (F3-F4, P3-P4; Philips et al., 2012), showing significantly smaller PLV for trans-hemispheric pairs ($p < 0.01$).

### 4. DISCUSSION

The major objective of the study was to explore the dynamic functional connectivity of fronto-parietal networks during visual perception in neglect patients. For that aim (1) inter-regional phase synchronization of event-related oscillatory activity was analyzed, and (2) a visuo-motor task was used, in which task relevance depended on integrated information from the two visual hemi-fields. To distinguish between dysfunctions produced by right-hemisphere lesions and by deficits in visual awareness, two groups of patients with right-hemisphere damage were studied, only one of which manifested left hemi-neglect. To evaluate processing of perceived stimuli, only correctly responded trials were analyzed.

According to major observations (1) The dynamic connectivity between frontal and parietal regions during visual perception was supported by two functional networks, an early one (around 120 ms) operating in the beta (15-25 Hz) frequency range, and a later one (around 160 ms) operating in the theta (4-8 Hz) frequency range. Activation in both networks was related to visual stimulus discrimination. (2) Neglect pathology was specifically associated with significant suppressions of both beta and theta networks engaging right parietal regions, which predicted additively hemi-neglect symptoms. (3) In contrast, beta connectivity was enhanced and theta connectivity was disrupted only in the left hemisphere in patients without neglect. (4) The functional involvement of both networks in stimulus discrimination was deviant in each of the two patient groups, but in different ways. These results confirm models according to which disrupted integrity of right-hemisphere fronto-parietal networks is a core pathophysiological mechanism in neglect syndrome (Corbetta and Shulman, 2011; Bartolomeo et al., 2012). So far, a disconnection of right fronto-parietal networks in neglect has been demonstrated at the neuroanatomical and neurofunctional level using in-vivo tractography (Thiebaut de Schotten et al., 2005, 2011), lesion mapping (Ptak and Schnider, 2010; Lunven et al., 2015), fMRI (He et al., 2007; Bartolomeo et al., 2012) and resting state networks analysis of MRI and EEG (Baldassarre et al., 2014; Fellrath et al., 2016). However, the role of transient functional synchronization as a network-based

22

mechanism underlying perceptual deficits in neglect has not been identified. The present results demonstrate for the first time that dynamic fronto-parietal interactions are impaired during early stages (within the first 200 ms) of visual perception in neglect pathology. Also, original evidence is provided that multiple stages of fronto-parietal dysfunction contribute independently to deficits in visual awareness at the behavioural level.

The predictive role of fronto-parietal interactions for BIT, in combination with the close-to-chance level of performance in neglect patients, shows that the findings from correct responses reflect deficient rather than compensatory processes in these patients. From a clinical point of view it is relevant to note that lesion size in patients did not predict perceptual problems captured by BIT. Also, most neglect patients had lesions in the right temporo-parietal and posterior parietal regions, in contrast to patients without neglect, implicating the role of these regions for synchronization-mediated visual perception.

Although phase synchronization computed here is independent of amplitude (Tallon-Baudry et al., 1997; Lachaux et al., 1999) several confounders of true inter-regional phase coupling still can be accounted for (Cohen, 2014, 2015). One major confounder is volume conduction, which has to be suspected especially when surface EEG signals were not spatially enhanced by Laplacian transformations (Kayser and Tenke, 2015). In the present study, no such transformation was applied due to the insufficient number of recording electrodes. Several approaches and control observations exclude critical effects of volume conduction. First, PLV measures were computed against a base-line to minimize effects of volume conduction and common (reference) sources. Second, most of the correlations between power values at frontal and parietal electrodes were negative or non-significant and total power never predicted PLV, making common-source or conducted power modulations on synchronizations implausible (Cohen, 2014; 2015). Third, our PLV results refer to between-condition differences rather than to absolute PLV, so that possible volume conduction affecting each condition would be cancelled out. Fourth, control analyses revealed that PLI,

another index of inter-regional synchronization (Stam et al., 2007; Cohen, 2015), which, however, is free of influences of volume conduction and common sources, predicted consistently PLV, thus confirming the essential contribution of true connectivity sources to the PLV measure. Furthermore, PLI analyses generally confirmed PLV findings, indicating that the two measures capture specific but related characteristics of inter-regional connectivity in patients with right-hemisphere damage.

Another confounder of PLV may come from inter-trial phase-alignment induced by the stimulus. In this case, stimulus-related oscillations can be generated at multiple regions independently and simultaneously. The PLV measure could have therefore reflected the synchronous generation of stimulus-induced theta and beta oscillations at frontal and parietal regions rather than the true connectivity between frontal and parietal regions. Analyses of PLF, a measure of local inter-trial phase-locking (Tallon-Baudry, 2007) did reveal maximal local synchronization at occipito-parietal regions. Analyses also demonstrated that theta PLF was indeed reduced in patients with right hemisphere damage, yet independently of the presence of neglect symptoms, which was not consistent with effects of pathology on PLV. Moreover, in contrast to beta PLV, beta PLF was not affected significantly by pathology. Additional comparisons of pairs grouped by a common electrode confirmed that PLV differences existed irrespective of the common link to a PLF-specific electrode. Also, PLI computation abolishes the contribution of fully synchronous oscillations to the final estimate, but was still predictive for PLV. Together, these observations demonstrate that distributed fronto-parietal processing indexed by inter-regional synchronization may be distinguished from local processing captured by power and phase modulations of event-related theta and beta oscillations.

4.1. Distinct theta and beta functional networks during visual perception

Several observations support the distinctiveness of beta and theta networks. (1) Data-driven evidence is provided by time-frequency analysis, which revealed two separable TF

components with distinct temporal features. (2) The functional architectures of synchronized beta and theta networks differed in controls: Specific node functions were detected for dorsal frontal and ventral parietal regions for theta networks, whereas no such region-specific synchronization were found for beta networks (Bressler and Menon, 2010). (3) The functional involvement of the two networks was different, because in controls, targets were associated with a prominent reduction of beta synchronization relative to non-targets, whereas opposite relations (increased synchronization to targets) were detected for theta. (4) The spatial localization of functionally reactive connections was specific for beta (right parietal), but not for theta synchronization in controls. (5) The effects of pathology were different: In contrast to the right-hemisphere suppression of PLV in neglect, beta synchronization was overall raised, especially at right parietal regions, and theta synchronization was decreased only in the left hemisphere in patients without neglect. Together, these observations demonstrate that specific functional mechanisms are represented by the early beta and late theta coupling between frontal and parietal regions in the process of visual perception (von Stein et al., 2000; Başar et al., 2001; Buzsáki, 2006). Further, these mechanisms appear to be affected differentially by right-hemisphere lesions, thus being differentially associated to the expression of clinical symptoms of neglect at the behavioural level.


4.2. Fronto-parietal beta synchronization during visual processing

In patients with neglect, the significant reduction of fronto-parietal beta synchronization was dominated by disrupted right parietal connections. The observation that beta PLV was increased in patients without neglect shows that reduced fronto-parietal beta connectivity can be linked to the behavioural expression of neglect pathology rather than to the existence of right-hemisphere damage per se. Furthermore, suppressed beta synchronization between right parietal and left frontal regions predicted the amount of deficits in visual awareness as reflected by clinical BIT scores. These observations reveal for the first time that impaired

functional synchronization of fronto-parietal beta networks at very early stages (around 120 ms) of visual stimulus processing may constitute one of the neural substrates of neglect pathology.

Various previous studies have documented the involvement of fronto-parietal beta networks in visual processing in different conditions (attentional blink, contour detection, object recognition, etc.). Hipp et al. (2011) have identified large scale beta synchronization in a distinctive network of frontal, parietal and extrastriate visual areas in relation to visual perceptual organization. Fronto-parietal synchrony in the beta band also has been associated with visual search (Buschman and Miller, 2007), integration of visual information and perceptual grouping (Srinivasan et al., 1999; Phillips and Takeda, 2009; Phillips et al., 2012; Volberg and Greenlee, 2014; Castellano et al., 2014), visual attention (Gross et al., 2004; Marois et al., 2000; Wróbel, 2000), and visual object recognition (Sehatpour et al., 2008; Castellano et al., 2014). These previous studies, however, point to the existence of ongoing fronto-parietal beta synchronization that modulates brain responses to visual input (Gross et al., 2004; Liang et al. 2002; Hipp et al., 2011), or beta synchrony at later stages (150-300 ms) of visual stimulus processing (Phillips et al., 2012; Sehatpour et al., 2008; Dehaene and Changeux, 2011).

The time, frequency and regional characteristics of beta networks analyzed here resemble those of visual gamma-band responses manifesting synchronization at 120 ms over occipito-posterior regions (rev. Martinovic and Busch, 2011). Due to double modulation by both visual stimulus properties and task requirements, evoked gamma activity has been hypothesized to reflect an early processing level where bottom-up stimulus representations interact directly with top-down influences (Busch et al., 2006; Martinovic and Busch, 2011). In contrast to the enhancing effect of task relevance predicted by this hypothesis, fronto-parietal beta synchronization in controls was significantly decreased for target relative to non-target stimuli. Hence, top-down attentional modulation of task relevant features may not be a

key mechanism supported by FP beta synchronization observed here, although task relevance may have been less efficient in substantiating differences at early stages of processing due to the delayed-response instruction.

Beta synchronization may have captured other interactive processes at early processing stages. One such process is access of sensory information to consciousness (Dehaene and Changeux, 2011) as implied by the disrupted fronto-parietal connectivity during anesthesia-induced loss of consciousness (Ferrarelli et al., 2010; Ku et al., 2011), early (80-130 ms) synchronization correlates of conscious detection (Melloni et al., 2007; Wyart et al., 2012), and currently found correlations with BIT scores in patients. However, the target-related decrease of beta synchronization in control participants contradicts this explanation.

In the present study, targets and non-targets differed with respect to congruency of information in the two visual hemi-fields, the binding of which is supported by inter-hemispheric phase synchronization (Mima et al., 2001). Sutoyo and Srinivasan (2009) have elicited enhanced responses to conscious binding of congruent information from complementary hemi-fields into a coherent percept. Although their findings cannot be directly linked to the present results, they strongly imply that early beta synchronization is sensitive to the integration of visual information from the two hemi-fields (Mima et al., 2001; Phillips and Takeda, 2009; Phillips et al., 2012; Busch et al., 2004; Castellano et al., 2014). As indicated by the stimulus-type effect in controls, binding congruent information into a coherent full-field percept is associated with stronger beta synchronization between right parietal and frontal regions, which, however, was specifically impaired in the N+ group (Fig. 4). This implies deficient integration of a coherent full-field percept in neglect.

Interestingly, right parietal and left frontal regions were identified by Gross et al. (2004) as critical for the functioning of a beta target-related network likely representing a state of increased sensitivity (higher vigilance). Exactly these pairs were pathologically enhanced in patients with right hemisphere lesion without neglect. Hence, arousal responses

involving left frontal regions during early stimulus detection may be abnormally raised in right-hemisphere damage without neglect, but may be critically compromised in neglect (Rastelli et al., 2013), as further suggested by the predictive value of this network for BIT scores in patients. With regard to the finding of Rastelli et al. (2013) that left frontal beta activity selectively precedes neglect-related omissions, our results suggest that this predictive value of left frontal beta depends on the synchronization of this activity with right parietal activity. Thus, visual integration in neglect may be impaired due to poor arousal/attention modulation (Corbetta and Shulman, 2011; Chica et al., 2012, 2014), or to disrupted interactions between integrated visual representations and the arousal system.

4.3. Fronto-parietal theta synchronization during visual processing

In contrast to beta, the organization and pathology-related aberrations of fronto-parietal theta networks followed a ventral/dorsal distinction. Moreover, major differences in patients were evident for within-hemispheric pairs, with the left dorsal connectivity being disrupted in the two patient groups, and the right dorsal connectivity being impaired only in patients with neglect. Also specific for neglect was the reduced synchronization of the ventral pairs grouped by parietal regions during non-target processing.

These dynamic and functional characteristics appear to correspond closely to the ventral and dorsal attention networks operating in the theta range identified by Daitch et al. (2013). Previous studies have found a consistent correlation between theta fronto-parietal synchronization and attentional processing in working memory tasks (Sauseng et al., 2005, 2010; Deiber et al., 2007), especially in the right hemisphere (Astle et al., 2015). Also, fronto-parietal theta activity has been linked to cognitive control and performance monitoring in association with working memory (Cohen, 2011; Gulbinaite et al., 2014). Notably, the timing of maximal FP theta synchronization observed here (around 160 ms after stimulus onset) is in the latency range of visual N1 ERP component where major effects of visual attention have

been consistently observed (Luck et al., 2000; Verleger et al., 1996; Herrmann and Knight, 2001). In the same latency range, event-related theta oscillations have been correlated with attention and working memory mechanisms during target discrimination (Yordanova et al., 2006). The current observation that theta PLV was increased during target processing is in line with these studies by indicating enhanced reactivity to task relevance. Hence, the fronto-parietal theta synchronization analyzed here appears associated with mechanisms of top-down control and may therefore capture the activation of attentional networks (Daitch et al., 2013).

In this perspective, the impairment of dorsal FP theta networks in neglect patients is consistent with the results of Ptak and Schnider (2010) identifying the dorsal networks as critical, as well as with most recent observations of Fellrath et al. (2106), according to which a significant decrease of resting-state theta EEG connectivity predicted impaired target processing in patients with spatial neglect. According to He et al. (2007), both dorsal and ventral attentional networks are impaired in acute patients with neglect (tested within 1 month after lesion). In chronic states (more than 6 months after lesion), the dorsal attentional network was found to be recovered, whereas the ventral attentional network remained dysfunctional (He et al., 2007). In our study, neglect patients were tested between 1 and 29 weeks (mean 14 weeks) after lesion. Thus, consistent with He et al. (2007), in acute and sub-chronic patients studied here, synchronizations of both dorsal and ventral networks were impaired. Critically, as supported by recent neuroanatomical findings (Lunven et al., 2015), the dysfunction of the right dorsal fronto-parietal pair was specific for neglect and predicted independently symptoms of hemi-neglect.

The observation that the left dorsal synchronization was impaired in the two patient groups irrespective of the presence of neglect symptoms shows that the mechanism through which a right-hemisphere lesion disrupts fronto-parietal theta coherence may not be necessarily linked to a disconnection between parietal and frontal regions. A functional dysregulation of fronto-parietal networks may occur via thalamo-cortical pathways (Saalmann

29

and Kastner, 2011; Saalmann et al., 2012; Zikopoulos and Barbas, 2006, 2007; Lakatos et al., 2008). Also, the impaired synchronization of the left dorsal fronto-parietal network may follow a dysbalance in inhibitory influences between homologous parietal regions in the two hemispheres (Battelli et al., 2009; Plow et al., 2014). A complex system of both intra-hemispheric and homologue inter-hemispheric inhibitory influences has been identified including dorsal and ventral parietal regions, as well as occipital and temporal areas (Plow et al., 2014). It has been demonstrated that continuous theta burst stimulation applied over the left posterior parietal cortex can suppress hyperexcitability of left-hemisphere fronto-parietal circuits, which reduces visuospatial deficits in neglect patients (Koch et al. 2012; Bonni et al., 2013). Current observations of increased inter-hemispheric synchronizations between parietal and occipital regions in patients (Fig. 3) are consistent with fMRI findings of He et al. (2007) as well as with the notion of lesion-induced disinhibition of the left parieto-occipital system (Plow et al., 2014).

The present results show, however, that the theta network is specifically affected. Also, they show that dysfunctional connectivity within the left hemisphere alone may not subserve neglect symptoms although it may contribute to the pathological mechanisms (Koch et al., 2012). It is possible that both the right and left dorsal fronto-parietal theta networks support visual awareness, such that when one of them is spared, as in patients without neglect, perceptual problems do not emerge. Alternatively, the simultaneous involvement of the two right-hemisphere fronto-parietal networks, ventral and dorsal, may be critical for the emergence of neglect symptoms (He et al., 2007; Corbetta and Shulman, 2011).


4.4. Fronto-parietal networks and perceptual deficits in neglect
The finding that two functionally distinct networks synchronize frontal and parietal regions in successive stages of early visual processing can be interpreted in the context of multiple feedback processes susbserving visual perception via top-down attentional or knowledge

representations (Melloni et al., 2011; Rees, 2013). Foxe and Simpson (2002) have shown that a widespread system of sensory, parietal, and prefrontal areas is activated within 50-80 ms following visual input, providing a time frame for the initiation of feedback processes from frontal and parietal regions onto sensory areas. Even activity within the early P1 and N1 ERP components is likely to reflect such top down influences from frontal and parietal areas (Foxe and Simpson, 2002; Di Russo et al., 2008). Beta and theta synchronizations may therefore reflect a sequence of top-down interactions during visual perception. Several pathological mechanisms may affect the sequence of abnormal interactions observed here in neglect. 1) Integrated sensory representations are not maintained by parieto-occipital networks so that they cannot subserve communication with multiple top-down modulation systems at the times of their transient activations after stimulation (Di Russo et al., 2008). 2) Such representations are formed (Rees, 2013) but are not accessible or not functional due to specific impairments in the arousal system (Corbetta and Shulman, 2011, Chica al., 2012). 3) The mere formation of top-down representations of spatial and feature-based information may be compromised, since attentional top-down representations engage frontal and parietal regions (Gross et al., 2004; Egner et al., 2008; Chica et al., 2013) and modulate subsequent perception (Hipp et al., 2011; Melloni et al., 2011; Wyart et al., 2012).

Current findings on visual ERP components show that the earlier fronto-parietal synchronization in the beta range (around 120 ms) takes place after the bottom-up activation of extrastriate cortex reflected here by P1 latency at around 90 ms while the late fronto-parietal synchronization in the theta range (around 160 ms) occurs during the reactivation of occipital visual areas due to top-down feedbacks as reflected by late N1 component (Di Russo et al., 1998). The preserved P1 component and deficient N1 component confirm the observation of Di Russo et al. (1998) indicating intact bottom-up activation and impaired re-activation of occipital visual areas in the right hemisphere in neglect pathology. Dynamic fronto-parietal synchronization reveals additional new mechanisms modulating early visual

processing in patients with lesions in the right hemisphere, with or without neglect symptoms. In view of existing neuroelectric indices of visual processing including also oscillatory visual responses and markers of cortical excitability, the interactions between fronto-parietal synchronizations and other perceptual and attention processes merit the focus of future research.

5. CONCLUSION

Fronto-parietal networks operating in beta and theta frequency ranges are synchronized at early stages (within 200 ms) of visual processing. They support independently different stages of visual processing. The disruption of transient synchronization of right-hemisphere fronto-parietal networks during early visual processing is a plausible neurofunctional substrate of visual awareness deficits in patients with left hemi-neglect syndrome.

## 6. REFERENCES

Astle DE, Luckhoo H, Woolrich M, Kuo BC, Nobre AC, Scerif G. The neural dynamics of fronto-parietal networks in childhood revealed using magnetoencephalography. Cereb Cortex 2015; 25(10): 3868-76.

Babiloni C, Vecchio F, Rossi S, De Capua A, Bartalini S, Ulivelli M, Rossini, PM. Human ventral parietal cortex plays a functional role on visuospatial attention and primary consciousness. A repetitive transcranial magnetic stimulation study. Cereb Cortex 2007; 17: 1486–1492.

Baldassarre A, Ramsey L, Hacker CL, Callejas A, Astafiev SV, Metcalf NV, Zinn K, Rengachary J, Snyder AZ, Carter AR, Shulman GL, Corbetta M. Large-scale changes in network interactions as a physiological signature of spatial neglect. Brain 2014; 137(Pt 12): 3267-83. doi: 10.1093/brain/awu297

Bartolomeo P, Thiebaut de Schotten M, Chica AB. Brain networks of visuospatial attention and their disruption in visual neglect. Front Hum Neurosci 2012; 6: 110.

Başar E, Başar-Eroglu C, Karakaş S, Schürmann M. Gamma, alpha, delta, and theta oscillations govern cognitive processes. Int J Psychophysiol 2001; 39(2-3): 241-8.

Battelli L, Alvarez GA, Carlson T, Pascual-Leone A. The role of the parietal lobe in visual extinction studied with transcranial magnetic stimulation. J Cogn Neurosci 2009; 21: 1946-55. doi:10.1162/jocn.2008.21149

Beck DM, Muggleton N, Walsh V, Lavie N. Right parietal cortex plays a critical role in change blindness. Cereb Cortex 2006; 16: 712–717.

Boehler CN, Schoenfeld MA, Heinze HJ, Hopf JM. Rapid recurrent processing gates awareness in primary visual cortex. Proc Natl Acad Sci USA 2008; 105: 8742-7. doi:10.1073/pnas.0801999105

Bonnì S, Mastropasqua C, Bozzali M, Caltagirone C, Koch G. Theta burst stimulation improves visuo-spatial attention in a patient with traumatic brain injury. Neurol Sci 2013; 34(11): 2053-6. doi: 10.1007/s10072-013-1412-y

Bressler SL, Menon V. Large-scale brain networks in cognition: emerging methods and principles. Trends Cogn Sci 2010; 14(6): 277-90. doi: 10.1016/j.tics.2010.04.004

Bressler SL, Tognoli E. Operational principles of neurocognitive networks. Int J Psychophysiol 2006; 60(2): 139-48.

Busch NA, Debener S, Kranczioch C, Engel AK, Herrmann CS. Size matters: effects of stimulus size, duration and eccentricity on the visual gamma-band response. Clin Neurophysiol 2004; 115(8): 1810-20.

Busch NA, Schadow J, Fruend I, Herrmann CS. Time-frequency analysis of target detection reveals an early interface between bottom-up and top-down processes in the gamma-band. NeuroImage 2006; 29: 1106–1116.

Buschman TJ, Miller EK. Top-down versus bottom-up control of attention in the prefrontal and posterior parietal cortices. Science 2007; 315(5820): 1860-2.

Buzsáki G. Rhythms of the brain. Oxford University Press, Inc.: New York; 2006.

Carmel D, Walsh V, Lavie N, Rees G. Right parietal TMS shortens dominance durations in binocular rivalry. Curr Biol 2010; 20: R799–R800.

Castellano M, Plöchl M, Vicente R, Pipa G. Neuronal oscillations form parietal/frontal networks during contour integration. Front Integr Neurosci 2014; 8:64. doi: 10.3389/fnint.2014.00064

Chica AB, Thiebaut de Schotten M, Toba M, Malhotra P, Lupiáñez J, Bartolomeo P. Attention networks and their interactions after right-hemisphere damage. Cortex 2012; 48: 654-63.

Chica AB, Paz-Alonso PM, Valero-Cabré A, Bartolomeo P. Neural bases of the interactions between spatial attention and conscious perception. Cereb Cortex 2013; 23(6): 1269-79. doi: 10.1093/cercor/bhs087

Chica AB, Thiebaut de Schotten M, Toba M, Malhotra P, Lupiáñez J, Bartolomeo P. Attention networks and their interactions after right-hemisphere damage. Cortex 2012; 48(6): 654-63. doi: 10.1016/j.cortex.2011.01.009

Cohen MX. Effects of time lag and frequency matching on phase-based connectivity. J Neurosci Methods 2015; 250: 137-46.

Cohen MX. Analyzing neural time series data: Theory and practice. The MIT Press: Cambridge, Massachusetts, 2014.

Cohen MX. Error-related medial frontal theta activity predicts cingulate-related structural connectivity. NeuroImage 2011; 55: 1373-83.

Corbetta M, Shulman GL. Control of goal-directed and stimulus-driven attention in the brain. Nat Rev Neurosci 2002; 3: 201-15.

Corbetta M, Shulman GL. Spatial neglect and attention networks. Annu Rev Neurosci 2011; 34: 569-99.

Daitch AL, Sharma M, Roland JL, Astafiev SV, Bundy DT, Gaona CM, Snyder AZ, Shulman GL, Leuthardt EC, Corbetta M. Frequency-specific mechanism links human brain networks for spatial attention. Proc Natl Acad Sci USA 2013; 110: 19585-90.

Damasio H, Damasio A. Lesion Analysis in Neuropsychology, Oxford University Press, New York 1989.

Dehaene S, Changeux JP. Experimental and theoretical approaches to conscious processing. Neuron 2011; 70(2): 200-27. doi: 10.1016/j.neuron.2011.03.018

Deiber MP, Missonnier P, Bertrand O, Gold G, Fazio-Costa L, Ibañez V, Giannakopoulos P. Distinction between perceptual and attentional processing in working memory tasks: a study of phase-locked and induced oscillatory brain dynamics. J Cogn Neurosci 2007; 19(1): 158-72.

Di Russo F, Aprile T, Spitoni G, Spinelli D. Impaired visual processing of contralesional stimuli in neglect patients: a visual-evoked potential study. Brain 2008; 131(Pt 3): 842-54.

Doricchi F, Tomaiuolo F. The anatomy of neglect without hemianopia: a key role for parietal-frontal disconnection? NeuroReport 2003; 14(17): 2239-43.

Driver J, Vuilleumier P. Perceptual awareness and its loss in unilateral neglect and extinction. Cognition 2001; 79: 39–88.

Egner T, Monti JM, Trittschuh EH, Wieneke CA, Hirsch J, Mesulam MM. Neural integration of top-down spatial and feature-based information in visual search. J Neurosci 2008; 28(24): 6141-51. doi: 10.1523/JNEUROSCI.1262-08.2008

Fellrath J, Mottaz A, Schnider A, Guggisberg AG, Ptak R. Theta-band functional connectivity in the dorsal fronto-parietal network predicts goal-directed attention. Neuropsychologia 2016; in press. doi: 10.1016/j.neuropsychologia.2016.07.012

Ferrarelli F, Massimini M, Sarasso S, Casali A, Riedner BA, Angelini G, Tononi G, Pearce RA. Breakdown in cortical effective connectivity during midazolam-induced loss of consciousness. Proc Natl Acad Sci USA 2010; 107: 2681-6. doi:10.1073/pnas.0913008107

Foxe JJ, Simpson GV. Flow of activation from V1 to frontal cortex in humans. A framework for defining "early" visual processing. Exp Brain Res 2002; 142(1): 139-50.

Fries P, Reynolds JH, Rorie AE, Desimone R. Modulation of oscillatory neuronal synchronization by selective visual attention. Science 2001; 291: 1560-3.

Fries P. A mechanism for cognitive dynamics: Neuronal communication through neuronal coherence. Trends Cogn Sci 2005; 9: 474-80.

Gratton G, Coles MGH, Donchin E. A new method for off-line removal of ocular artifact. Electroencephalogr Clin Neurophysiol 1983; 55: 468-84.

Gross J, Schmitz F, Schnitzler I, Kessler K, Shapiro K, Hommel B, Schnitzler A. Modulation of long-range neural synchrony reflects temporal limitations of visual attention in humans. Proc Natl Acad Sci USA 2004; 101(35): 13050-5.

Gulbinaite R, van Rijn H, Cohen MX. Fronto-parietal network oscillations reveal relationship between working memory capacity and cognitive control. Front Hum Neurosci 2014; 8:761. doi: 10.3389/fnhum.2014.00761

Hardwick RM, Rottschy C, Miall RC, Eickhoff SB. A quantitative meta-analysis and review of motor learning in the human brain. NeuroImage 2013; 67: 283-97. doi: 10.1016/j.neuroimage.2012.11.020

He BJ, Snyder AZ, Vincent JL, Epstein A, Shulman GL, Corbetta M. Breakdown of functional connectivity in frontoparietal networks underlies behavioral deficits in spatial neglect. Neuron 2007; 53: 905-18.

Herrmann CS, Knight RT. Mechanisms of human attention: event-related potentials and oscillations. Neurosci Biobehav Rev 2001; 25(6): 465-76.

Hillis AE. Neurobiology of unilateral spatial neglect. Neuroscientist 2006; 12: 153-63.

Hipp JF, Engel AK, Siegel M. Oscillatory synchronization in large-scale cortical networks predicts perception. Neuron 2011; 69(2): 387-96. doi: 10.1016/j.neuron.2010.12.027

Husain M, Kennard C. Visual neglect associated with frontal lobe infarction. J Neurol 1996; 243: 652-7.

Husain M, Rorden C. Non-spatially lateralized mechanisms in hemispatial neglect. Nat Rev Neurosci 2003; 4: 26-36.

Kayser J, Tenke CE. Issues and considerations for using the scalp surface Laplacian in EEG/ERP research: A tutorial review. Int J Psychophysiol 2015; 97(3): 189-209. doi: 10.1016/j.ijpsycho.2015.04.012

Kanai R, Muggleton NG, Walsh V. TMS over the intraparietal sulcus induces perceptual fading. J Neurophysiol 2008; 100: 3343–3350.

Karnath HO, Fruhmann Berger M, Küker W, Rorden C. The anatomy of spatial neglect based on voxelwise statistical analysis: a study of 140 patients. Cereb Cortex 2004; 14: 1164-72.

Kihara K, Ikeda T, Matsuyoshi D, Hirose N, Mima T, Fukuyama H, Osaka N. Differential contributions of the intraparietal sulcus and the inferior parietal lobe to attentional blink: Evidence from transcranial magnetic stimulation. J Cogn Neurosci 2011; 23: 247–256.

Koch G, Bonnì S, Giacobbe V, Bucchi G, Basile B, Lupo F, Versace V, Bozzali M, Caltagirone C. θ-burst stimulation of the left hemisphere accelerates recovery of hemispatial neglect. Neurology 2012; 78(1): 24-30. doi: 10.1212/WNL.0b013e31823ed08f

Koivisto M, Grassini S. Neural processing around 200 ms after stimulus-onset correlates with subjective visual awareness. Neuropsychologia 2016; 84: 235-43.

Ku SW, Lee U, Noh GJ, Jun IG, Mashour GA. Preferential inhibition of frontal-to-parietal feedback connectivity is a neurophysiologic correlate of general anesthesia in surgical patients. PLoS One 2011; 6: e25155. doi:10.1371/journal.pone.0025155

Lakatos P, Karmos G, Mehta AD, Ulbert I, Schroeder CE. Entrainment of neuronal oscillations as a mechanism of attentional selection. Science 2008; 320: 110-3.

Lachaux JP, Rodriguez E, Martinerie J, Varela FJ. Measuring phase synchrony in brain signals. Hum Brain Mapp 1999; 8(4): 194-208.

Liang H, Bressler SL, Ding M, Truccolo WA, Nakamura R. Synchronized activity in prefrontal cortex during anticipation of visuomotor processing. NeuroReport 2002; 13(16): 2011-5.

Luck SJ, Woodman GF, Vogel EK. Event-related potential studies of attention. Trends Cogn Sci 2000; 4(11): 432-440.

Lunven M, Thiebaut De Schotten M, Bourlon C, Duret C, Migliaccio R, Rode G, Bartolomeo P. White matter lesional predictors of chronic visual neglect: a longitudinal study. Brain 2015; 138(Pt 3): 746-60. doi: 10.1093/brain/awu389

Mallat S. A Wavelet tour of signal processing, 2nd ed. San Diego: Academic Press; 1999.

Marois R, Chun MM, Gore JC. Neural correlates of the attentional blink. Neuron 2000; 28(1): 299-308.

Martinovic J, Busch NA. High frequency oscillations as a correlate of visual perception. Int J Psychophysiol 2011; 79(1): 32-8. doi: 10.1016/j.ijpsycho.2010.07.004

Melloni L, Schwiedrzik CM, Müller N, Rodriguez E, Singer W. Expectations change the signatures and timing of electrophysiological correlates of perceptual awareness. J Neurosci 2011; 31(4): 1386-96. doi: 10.1523/JNEUROSCI.4570-10.2011

Melloni L, Molina C, Pena M, Torres D, Singer W, Rodriguez E. Synchronization of neural activity across cortical areas correlates with conscious perception. J Neurosci 2007; 27: 2858-65.

Menon V. Developmental pathways to functional brain networks: emerging principles. Trends Cogn Sci 2013; 17(12): 627-40. doi: 10.1016/j.tics.2013.09.015

Mima T, Oluwatimilehin T, Hiraoka T, Hallett M. Transient interhemispheric neuronal synchrony correlates with object recognition. J Neurosci 2001; 21(11): 3942-8.

Mort DJ, Malhotra P, Mannan SK, Rorden C, Pambakian A, Kennard C, Husain M. The anatomy of visual neglect. Brain 2003; 126: 1986-97.

Petrides M, Pandya DN. Projections to the frontal cortex from the posterior parietal region in the rhesus monkey. J Comp Neurol 1984; 228: 105-16.

Phillips S, Takeda Y. Greater frontal-parietal synchrony at low gamma-band frequencies for inefficient than efficient visual search in human EEG. Int J Psychophysiol 2009; 73(3): 350-4. doi: 10.1016/j.ijpsycho.2009.05.011

Phillips S, Takeda Y, Singh A. Visual feature integration indicated by pHase-locked frontal-parietal EEG signals. PLoS One 2012; 7(3): e32502. doi:10.1371/journal.pone.0032502

Plow EB, Cattaneo Z, Carlson TA, Alvarez GA, Pascual-Leone A, Battelli L. The compensatory dynamic of inter-hemispheric interactions in visuospatial attention revealed using rTMS and fMRI. Front Hum Neurosci 2014; 8:226. doi: 10.3389/fnhum.2014.00226

Ptak R, Schnider A. The dorsal attention network mediates orienting toward behaviorally relevant stimuli in spatial neglect. J Neurosci 2010; 30: 12557-65.

Ptak R. The frontoparietal attention network of the human brain: action, saliency, and a priority map of the environment. Neuroscientist 2012; 18(5): 502-15.

Rastelli F, Tallon-Baudry C, Migliaccio R, Toba MN, Ducorps A, Pradat-Diehl P, Duret C, Dubois B, Valero-Cabré A, Bartolomeo P. Neural dynamics of neglected targets in

patients with right hemisphere damage. Cortex 2013; 49(7): 1989-96. doi: 10.1016/j.cortex.2013.04.001

Rees G. Neural correlates of consciousness. Ann NY Acad Sci 2013; 1296: 4-10. doi:10.1111/nyas.12257

Rodriguez E, George N, Lachaux JP, Martinerie J, Renault B, Varela FJ. Perception's shadow: long-distance synchronization of human brain activity. Nature 1999; 397: 430-3.

Roelfsema PR, Lamme VA, Spekreijse H. Synchrony and covariation of firing rates in the primary visual cortex during contour grouping. Nat Neurosci 2004; 7(9): 982-91

Rottschy C, Langner R, Dogan I, Reetz K, Laird AR, Schulz JB, Fox PT, Eickhoff SB. Modelling neural correlates of working memory: a coordinate-based meta-analysis. NeuroImage 2012; 60(1): 830-46. doi: 10.1016/j.neuroimage.2011.11.050

Rottschy C, Caspers S, Roski C, Reetz K, Dogan I, Schulz JB, Zilles K, Laird AR, Fox PT, Eickhoff SB. Differentiated parietal connectivity of frontal regions for "what" and "where" memory. Brain Struct Funct 2013; 218(6): 1551-67. doi: 10.1007/s00429-012-0476-4

Rounis E, Maniscalco B, Rothwell JC, Passingham R, Lau H. Theta-burst transcranial magnetic stimulation to the prefrontal cortex impairs metacognitive visual awareness. Cogn Neurosci 2010; 1: 165–175.

Saalmann YB, Kastner S. Cognitive and perceptual functions of the visual thalamus. Neuron 2011; 71: 209-23.

Saalmann YB, Pinsk MA, Wang L, Li X, Kastner S. The pulvinar regulates information transmission between cortical areas based on attention demands. Science 2012; 337: 753-6.

Sack AT. Using non-invasive brain interference as a tool for mimicking spatial neglect in healthy volunteers. Restor Neurol Neurosci 2010; 28(4): 485-97. doi: 10.3233/RNN-2010-0568

Sauseng P, Klimesch W, Schabus M, Doppelmayr M. Fronto-parietal EEG coherence in theta and upper alpha reflect central executive functions of working memory. Int J Psychophysiol 2005; 57(2) :97-103.

Sauseng P, Griesmayr B, Freunberger R, Klimesch W. Control mechanisms in working memory: a possible function of EEG theta oscillations. Neurosci Biobehav Rev 2010; 34(7): 1015-22. doi: 10.1016/j.neubiorev.2009.12.006

Schmahmann JD, Pandya DN. Fiber pathways of the brain. NewYork: Oxford University Press; 2006.

Sehatpour P, Molholm S, Schwartz TH, Mahoney JR, Mehta AD, Javitt DC, Stanton PK, Foxe JJ. A human intracranial study of long-range oscillatory coherence across a frontal-occipital-hippocampal brain network during visual object processing. Proc Natl Acad Sci USA 2008; 105(11): 4399-404. doi: 10.1073/pnas.0708418105

Srinivasan R, Russell DP, Edelman GM, Tononi G. Increased synchronization of neuromagnetic responses during conscious perception. J Neurosci 1999; 19(13): 5435-48.

Stam CJ, Nolte G, Daffertshofer A. Phase lag index: assessment of functional connectivity from multi channel EEG and MEG with diminished bias from common sources. Hum Brain Mapp 2007; 28(11): 1178-93.

Sumner P, Tsai PC, Yu K, Nachev P. Attentional modulation of sensorimotor processes in the absence of perceptual awareness. Proc Natl Acad Sci USA 2006; 103: 10520-5.

Sutoyo D, Srinivasan R. Nonlinear SSVEP responses are sensitive to the perceptual binding of visual hemifields during conventional 'eye' rivalry and interocular 'percept' rivalry. Brain Res 2009; 1251: 245-55. doi: 10.1016/j.brainres.2008.09.086

Tallon-Baudry C, Bertrand O, Delpuech C, Permier J. Oscillatory gamma-band (30– 70 Hz) activity induced by a visual search task in humans. J Neurosci 1997; 17: 722-34.

Thiebaut de Schotten M, Dell'acqua F, Forkel SJ, Simmons A, Vergani F, Murphy DGM, Catani M. A lateralized brain network for visuospatial attention. Nat Neurosci 2011; 14: 1245-6.

Thiebaut de Schotten M, Urbanski M, Duffau H, Volle E, Levy R, Dubois B, Bartolomeo P. Direct evidence for a parietal-frontal pathway subserving spatial awareness in humans. Science 2005; 309: 2226-8.

Tononi G, Koch C. The neural correlates of consciousness: an update. Ann NY Acad Sci 2008; 1124: 239-61. doi:10.1196/annals.1440.004

Tsuchiya N, Koch C. The relationship between consciousness and attention. In: Tononi G, Laureys S, editors. The neurology of consciousness. Oxford: Elsevier Academic; 2008. p. 63-77.

Vallar G, Perani D. The anatomy of unilateral neglect after right hemisphere stroke lesions: a clinical/CT-scan correlation study in man. Neuropsychologia 1986; 24: 609-22.

Vallar G, Rusconi ML, Bignamini L, Geminiani G, Perani D. Anatomical correlates of visual and tactile extinction in humans: a clinical CT scan study. J Neurol Neurosurg Psychiatry 1994; 57: 464-70.

van Boxtel JJ, Tsuchiya N, Koch C. Consciousness and attention: on sufficiency and necessity. Front Psychol 2010; 1: 217. doi:10.3389/fpsyg.2010.00217

Varela F, Lachaux JP, Rodriguez E, Martinerie J. The brainweb: phase synchronization and large-scale integration. Nat Rev Neurosci 2001; 2: 229-39.

Verleger R, Heide W, Butt C, Wascher E, Kömpf D. On-line brain potential correlates of right parietal patients' attentional deficit. Electroencephalogr Clin Neurophysiol 1996; 99(5): 444-57.

Vinck M, Oostenveld R, van Wingerden M, Battaglia F, Pennartz CM. An improved index of phase-synchronization for electrophysiological data in the presence of volume-conduction, noise and sample-size bias. NeuroImage 2011; 55(4): 1548-65.

Volberg G, Greenlee MW. Brain networks supporting perceptual grouping and contour selection. Front Psychol 2014; 5:264. doi: 10.3389/fpsyg.2014.00264

von Stein A, Chiang C, König P. Top-down processing mediated by interareal synchronization. Proc Natl Acad Sci USA 2000; 97: 14748-53.

Vuilleumier P, Schwartz S, Verdon V, Maravita A, Hutton C, Husain M, Driver J. Attention-dependent functional abnormality in retinotopic visual cortex for patients with parietal lesions and spatial neglect. Curr Biol 2008; 18(19): 1525–1529. doi:10.1016/j.cub.2008.08.072

Vuilleumier PO, Rafal RD. A systematic study of visual extinction. Between- and within-field deficits of attention in hemispatial neglect. Brain 2000;123:1263-79.

Wilson B, Cockburn J, Halligan PW. Behavioural inattention test. Titchfield, Hants: Thames Valley Press; 1987. (German version: Fels M, Geissner E. Neglect-Test. Göttingen: Hogrefe; 1997)

Wróbel A. Beta activity: a carrier for visual attention. Acta Neurobiol Exp (Wars) 2000; 60(2): 247-60.

Wyart V, Dehaene S, Tallon-Baudry C. Early dissociation between neural signatures of endogenous spatial attention and perceptual awareness during visual masking. Front Hum Neurosci 2012; 6: 16. doi:10.3389/fnhum.2012.00016

Wyart V, Tallon-Baudry C. Neural dissociation between visual awareness and spatial attention. J Neurosci 2008; 28: 2667-79. doi:10.1523/JNEUROSCI.4748-07.2008

Yordanova J, Heinrich H, Kolev V, Rothenberger A. Increased event-related theta activity as a psychophysiological marker of comorbidity in children with tics and attention-deficit/hyperactivity disorders. NeuroImage 2006; 32(2): 940-55.

Zikopoulos B, Barbas H. Circuits for multisensory integration and attentional modulation through the prefrontal cortex and the thalamic reticular nucleus in primates. Rev Neurosci 2007; 18: 417-38.

Zikopoulos B, Barbas H. Prefrontal projections to the thalamic reticular nucleus form a unique circuit for attentional mechanisms. J Neurosci 2006; 26: 7348-61.

Table 1. Information about patients with and without neglect. All lesions were in the right hemisphere.

| Patient | Age/sex | (Pre)-frontal lesions | (Pre)-central lesions | Posterior-parietal lesions | Lesions of the temporo-parietal junction | Temporal lobe lesions | Occipital lesions | Basal ganglia lesions | Pyramidal tract/internal capsule lesions | BIT | Lesion-to-test interval (weeks) |
|---|---|---|---|---|---|---|---|---|---|---|---|
| (a) Patients with neglect (N+) | | | | | | | | | | | |
| 1 | 72/f | | | ++ | ++ | | | | + | 116 | 11 |
| 2 | 78/f | | | ++ | +++ | | | | | 156 | 29 |
| 3 | 50/f | | + | ++ | + | | | ++ | | 125 | n.a. |
| 4 | 47/m | + | +++ | +++ | | | | | | 149 | 7 |
| 5 | 77/m | | | | ++ | | ++ (h) | ++ | + | 84 | 6 |
| 6 | 68/m | ++ | ++ | | ++ | | | | | 151 | 1 |
| 7 | 60/f | | ++ | + | ++ | | | ++ | | 148 | 13 |
| 8 | 35/m | +++ | +++ | +++ | +++ | | | +++ | +++ | 160 | 22 |
| 9 | 51/m | ++ | +++ | ++ | ++ | ++ | | + | | 154 | n.a. |
| (b) Patients with lesions without neglect (N-) | | | | | | | | | | | |
| 1 | 52/m | +++ | + | | | +++ | | | ++ | 168.5 | 28 |
| 2 | 58/f | | | | | ++ | | ++ | ++ | 170 | 12 |
| 3 | 55/f | + | | | | + | | ++ | + | 169 | 13 |
| 4 | 60/f | | | | | ++ | | + | ++ | 168.5 | 23 |
| 5 | 50/f | | | | | | | ++ | ++ | 169 | 12 |
| 6 | 68/f | ++ | + | | | | | | + | 168 | 24 |
| 7 | 62/m | ++ (sh) | | | | + | | | | 169.5 | 6 |
| 8 | 72/m | | + | | | + | | ++ | | 169.5 | 40 |
| 9 | 60/m | ++ | | | | | | | | 169.5 | 5 |
| 10 | 62/m | | | | | + | | ++ | | 169.5 | 6 |
| 11 | 61/m | + | + | | | | | | | 169 | 13 |

BIT, Behavioral Inattention Test (scores 167–170, no neglect; 136–166, moderate neglect; 73–135, severe neglect); +, minor involvement by the lesion; ++, partial involvement by the lesion; +++, complete involvement by the lesion; (h), hemorrhage; (sh), minor secondary hemorrhage; n.a., not available.

FIGURE LEGENDS


**Figure 1.** Illustration of the sinusoidal gratings stimuli used in the experiment, non-targets and targets.

**Figure 2.** Identification of time-frequency parameters. (A) Grand average time-frequency plots of PLV for fronto-parietal channel combinations pooled together in controls (CONTR), patients without neglect (N-), and patients with neglect (N+). (B) Temporal dynamics of inter-regional synchronization for all pair combinations in the three groups. Presented are extracted PLV scales in beta (15-25 Hz) and theta (4-8 Hz) frequency ranges. Fronto-parietal pairs are shown in red. PLV of non-target stimuli are shown.

**Figure 3.** Statistical results of the distribution of PLV across groups for classes of pairs. All 78 electrode pairs were grouped into 10 classes according to anatomical cortical regions shown at the top: fronto-frontal (FF), fronto-central (FC), fronto-parietal (FP), fronto-occipital (FO), centro-central (CC), centro-parietal (CP), centro-occipital (CO), parieto-parietal (PP), parieto-occipital (PO), and occipito-occipital (OO). For each class, the outcome of the $\chi^2$ statistical evaluation is presented, with the results corrected for multiple tests using Bonferroni procedure. The distribution is normalized and presented in percent.

   d*f,* degrees of freedom; *p*, significance of difference; *corr. p*, *p* corrected after Bonferroni procedure; \*\*, p < 0.01; \*\*\*, p < 0.001; *ns*, not significant; CONTR, controls; N-, patients without neglect; N+, patients with neglect.

**Figure 4.** Results of PLV time–frequency analysis for the beta range. (A) Grand average inter-electrode plots of beta PLV for all fronto-parietal pair combinations in three groups of participants – controls (CONTR), patients without neglect (N-), and patients with neglect (N+) for non-targets (NT), targets (T) and target minus non-target (T - NT) difference. Frontal (x-axis) and parietal (y-axis) electrodes over the left and right hemisphere are presented. Electrode pairs with significant differences between targets and non-targets are designated with asterisks. (B) Fronto-parietal pairs with significant beta PLV differences between control and N+ groups (CONTR – [N+]), patient groups without and with neglect ([N-]-[N+], and control and N- groups (CONTR - [N-]). Red color indicates higher values for the first than the second group, blue color – the opposite.

**Figure 5.** Results of PLV time–frequency analysis for the theta range. (A) Grand average inter-electrode plots of theta PLV for all fronto-parietal pair combinations in three groups of participants – controls (CONTR), patients without neglect (N-), and patients with neglect (N+) for non-targets (NT), targets (T) and target minus non-target (T - NT) difference. Frontal (x-axis) and parietal (y-axis) electrodes over the left and right hemisphere are designated. Electrode pairs with significant differences between targets and non-targets are designated with asterisks. (B) Group mean fronto-parietal pairs (F7-P7, F3-P3, F4-P4, and F8-P8) of theta PLV for control, N-, and N+ groups for non-targets (brighter colors) and targets (darker colors).
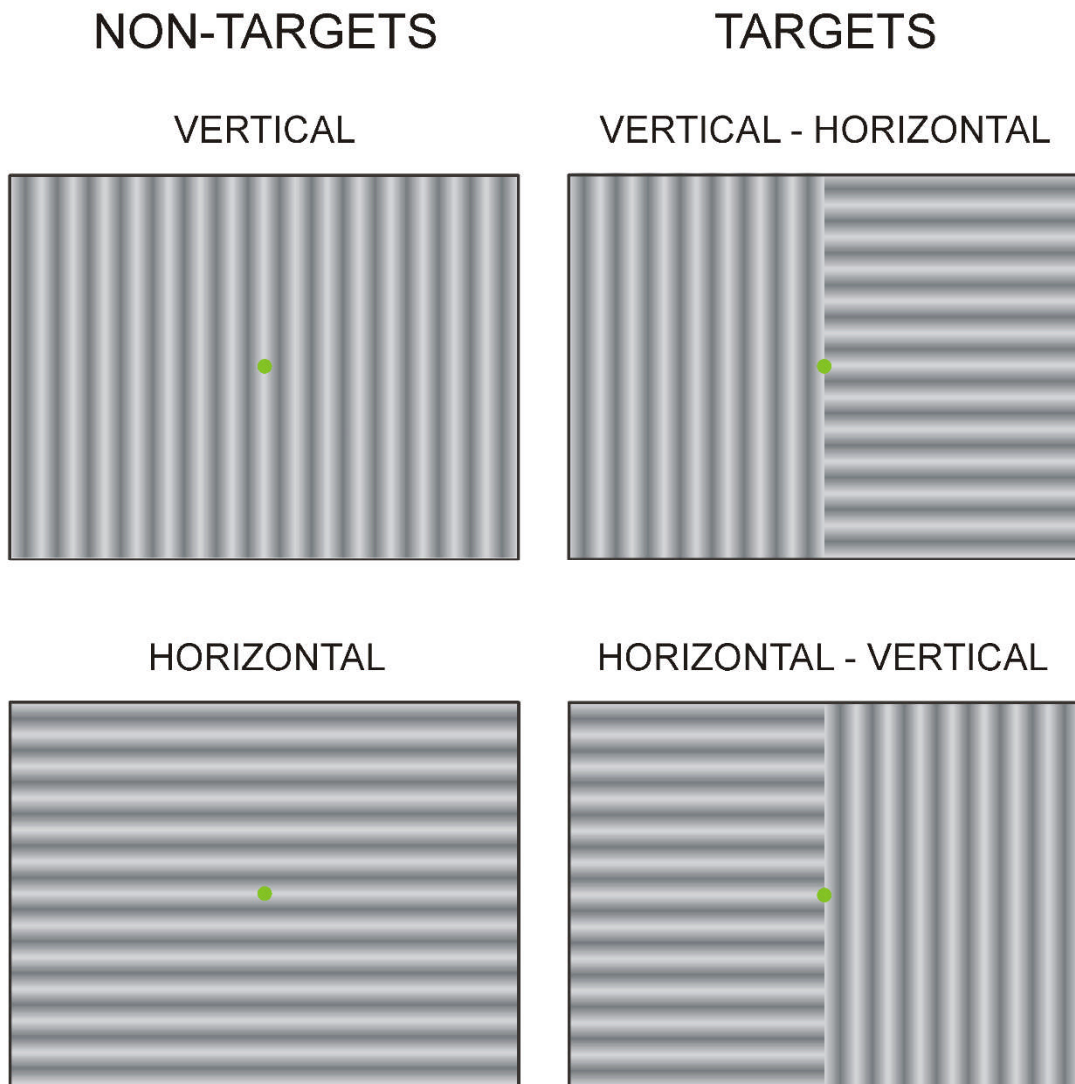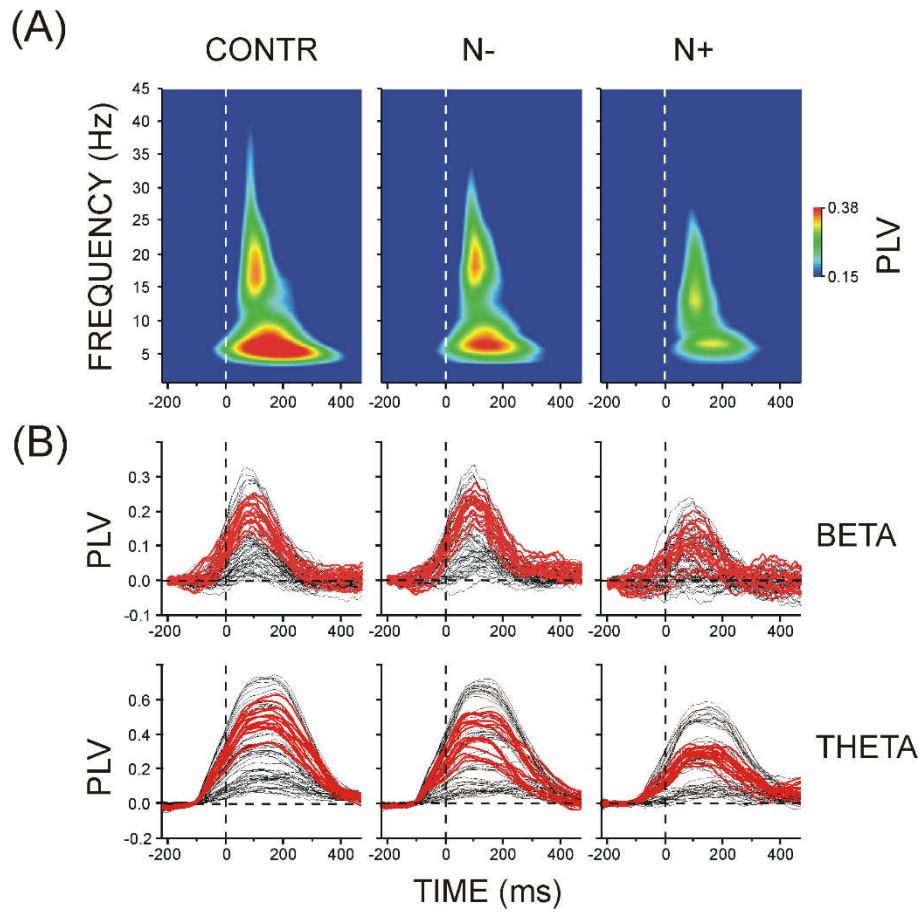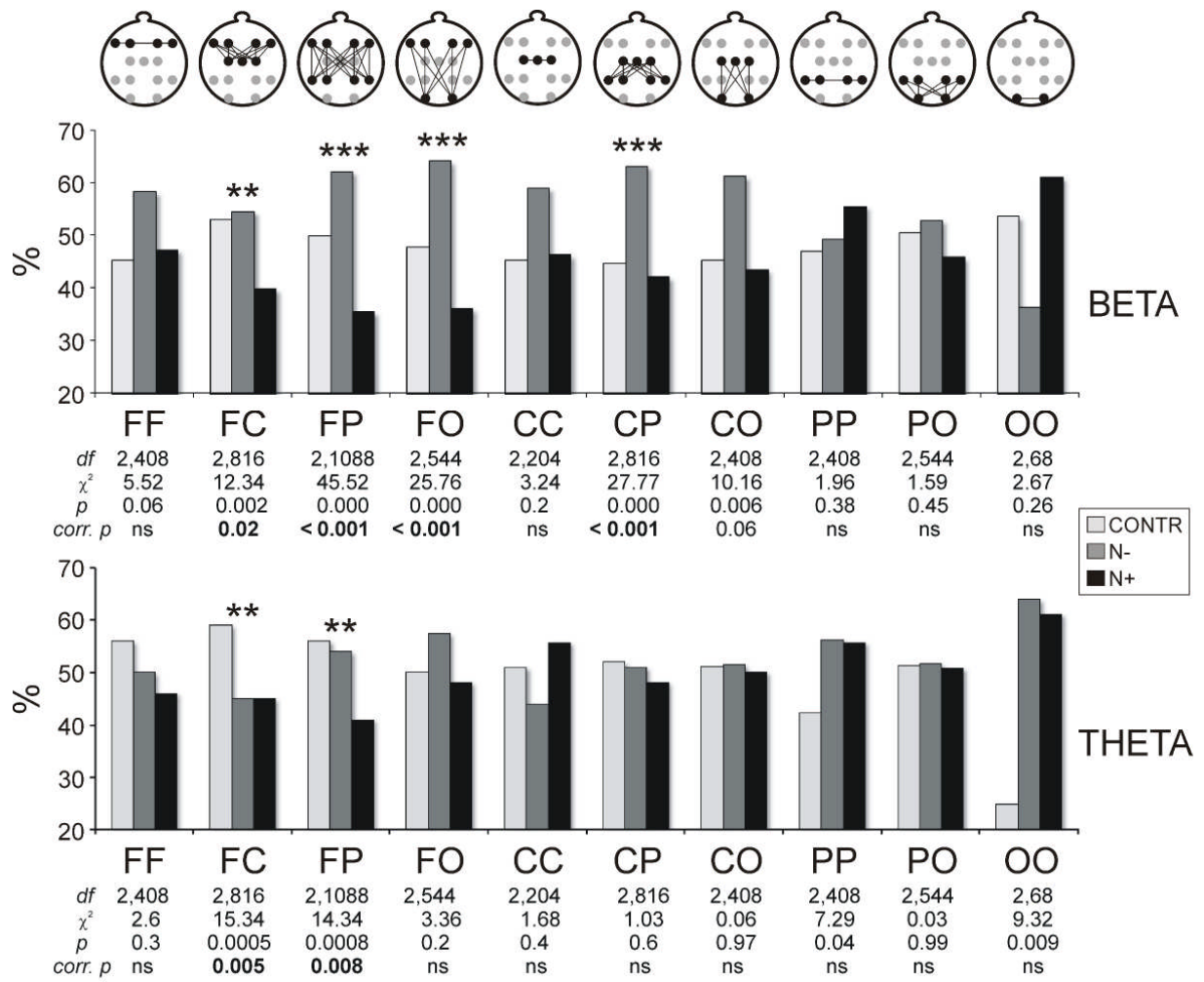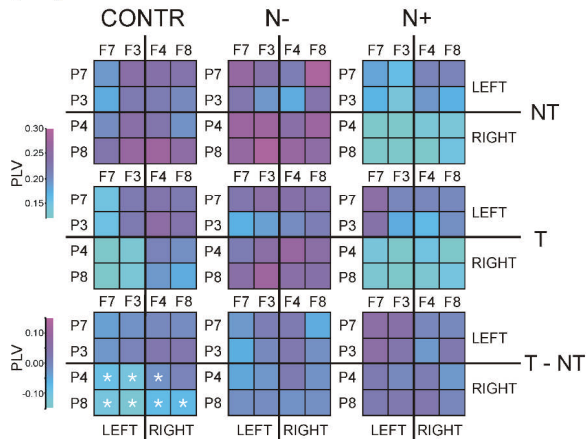
Fig. 1



NON-TARGETS

VERTICAL

HORIZONTAL

TARGETS

VERTICAL - HORIZONTAL

HORIZONTAL - VERTICAL

Fig. 2

Fig. 3



BETA

| | FF | FC | FP | FO | CC | CP | CO | PP | PO | OO |
|---|---|---|---|---|---|---|---|---|---|---|
| *df* | 2,408 | 2,816 | 2,1088 | 2,544 | 2,204 | 2,816 | 2,408 | 2,408 | 2,544 | 2,68 |
| $\chi^2$ | 5.52 | 12.34 | 45.52 | 25.76 | 3.24 | 27.77 | 10.16 | 1.96 | 1.59 | 2.67 |
| *p* | 0.06 | 0.002 | 0.000 | 0.000 | 0.2 | 0.000 | 0.006 | 0.38 | 0.45 | 0.26 |
| *corr. p* | ns | **0.02** | **< 0.001** | **< 0.001** | ns | **< 0.001** | 0.06 | ns | ns | ns |

THETA

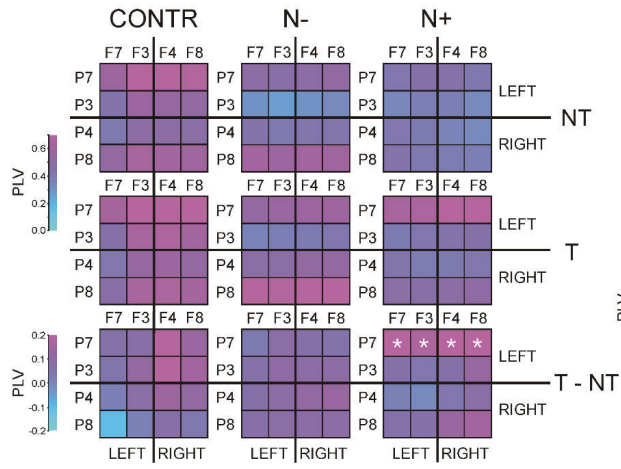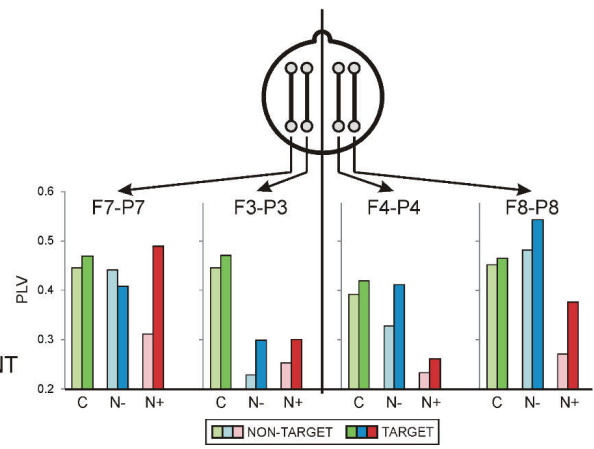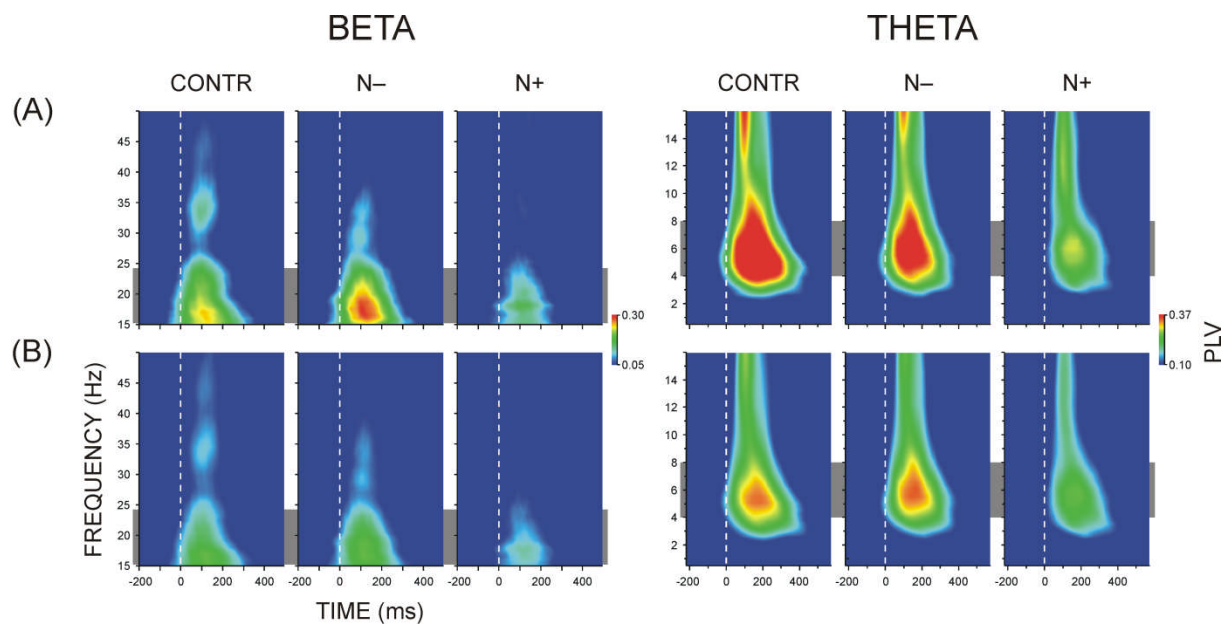| | FF | FC | FP | FO | CC | CP | CO | PP | PO | OO |
|---|---|---|---|---|---|---|---|---|---|---|
| *df* | 2,408 | 2,816 | 2,1088 | 2,544 | 2,204 | 2,816 | 2,408 | 2,408 | 2,544 | 2,68 |
| $\chi^2$ | 2.6 | 15.34 | 14.34 | 3.36 | 1.68 | 1.03 | 0.06 | 7.29 | 0.03 | 9.32 |
| *p* | 0.3 | 0.0005 | 0.0008 | 0.2 | 0.4 | 0.6 | 0.97 | 0.04 | 0.99 | 0.009 |
| *corr. p* | ns | **0.005** | **0.008** | ns | ns | ns | ns | ns | ns | ns |

CONTR
N-
N+

Fig. 4



(A)

(B)

Fig. 5

**Suppl. Fig. 1.**

    (A) Grand average time-frequency plots of PLV for fronto-parietal channel combinations pooled together in controls (CONTR), patients without neglect (N-), and patients with neglect (N+). TF decompositions are adapted to optimize the extraction of components in slow (< 15 Hz) and fast (>15 Hz) frequency bands. Separate beta and theta TF components are clearly observed in all groups. Following the optimal decomposition of fast-frequency components, a fast-frequency component in the gamma range (30-35 Hz) is expressed in controls.

    (B) Grand average time-frequency plots of global PLV for all 78 pair combinations pooled together in controls, N-, and N+ patients. Clear dominating components were expressed between 15 and 25 Hz within 200 ms and between 4 and 8 Hz Hz within 400 ms after stimulus in all groups. No significant between-group differences were yielded (beta, $F(2/31) = 1.48$, $p > 0.2$; theta, $F(2/31) = 0.5$, $p = 0.6$), although N+ patients displayed an overall reduction.

**Supplementary Material 2 (S2)**

Theta PLV of each group (controls, N-, and N+) was subjected to a Stimulus x Lat-F x Lat-P x DV-F x DV-P ANOVA. The following group-specific results were yielded.

    <u>Controls.</u> Although theta PLV during both target and non-target processing was pronounced for all FP pairs in controls, specific grouping by ventral parietal sites P7 and P8 was observed, pointing to local synchronizing functions of these regions – Fig. 5 (main text). PLV of pairs at P7 and P8 electrodes was significantly larger than PLV of pairs at P3 and P4 (DV-P, $F(1/13) = 9.64$, $p = 0.008$) verifying an enhanced local role for ventral parietal regions in mediating FP theta synchronization with all frontal regions. Also, PLV was significantly stronger for pairs at dorsal than ventral frontal electrodes (DV-F, $F(1/13) = 17.03$, $p < 0.001$) pointing to an increased local engagement of frontal dorsal regions in maintaining synchronization with parietal regions. Notably, the right ventral frontal region (F8) in controls also supported prominently the synchronization with all parietal regions, in contrast to the left ventral region (DV-F x Lat-F, $F(1/13) = 8.9$, $p = 0.01$). The main or interactive effects of Stimulus were not significant.

Patients without neglect. Similar to controls, theta PLV in N- patients did not depend on stimulus ($F(1/10) = 1.98$, $p = 0.2$). Opposite to controls, however, dorsal frontal regions did not manifest enhanced synchronizations with parietal regions (DV-F, $F(1/10) = 0.003$, $p > 0.95$). As demonstrated in Fig. 5 (main text), the dominating synchronizing properties of ventral parietal regions P7 and P8 were preserved (DV-P, $F(1/10) = 6.8$, $p = 0.03$). Confirming previous tests, the left dorso-parietal region at P3 in N- patients manifested a specific reduction of synchronization with all frontal regions (DV-F x DV-P x Lat-P, $F(1/10) = 6.2$, $p = 0.03$), which was particularly expressed for the synchronization with the dorsal frontal region F3 within the left hemisphere (DV-F x DV-P x Lat-F x Lat-P, $F(1/10) = 5.7$, $p = 0.04$).

Patients with neglect. As demonstrated in Fig. 5 (main text), only in neglect patients was non-target processing accompanied by a substantial reduction of FP theta synchronization as compared to target processing (Stimulus, $F(1/8) = 6.5$, $p = 0.03$). Although in N+ patients PLV was preserved during target processing, the pattern was deviant. It was determined by a preserved regional synchronization of ventral parietal sites (DV-P, $F(1/8) = 8.8$, $p = 0.02$; Stimulus x DV-P $F(1/8) = 6.6$, $p = 0.03$), predominantly on the left (P7; Stimulus x Lat-P, $F(1/8) = 9.1$, $p = 0.02$). However, both left and right dorsal pairs F3-P3 and F4-P4 manifested a reduction during both target and non-target processing, opposite to ventral parietal pairs (Stimulus x DV-F x DV-P x Lat-F x Lat-P, $F(1/8) = 5.2$, $p = 0.05$). As found in N- patients, dorsal frontal regions in the N+ group did not support a stronger synchronization with parietal regions as compared to ventral frontal regions (DV-F, $F(1/8) = 0.002$, $p > 0.7$), with synchronization with right parietal regions being most affected (VD-F x Lat-P, ($F(1/8) = 10.3$, $p = 0.01$).

**Supplementary Material 3 (S3)**
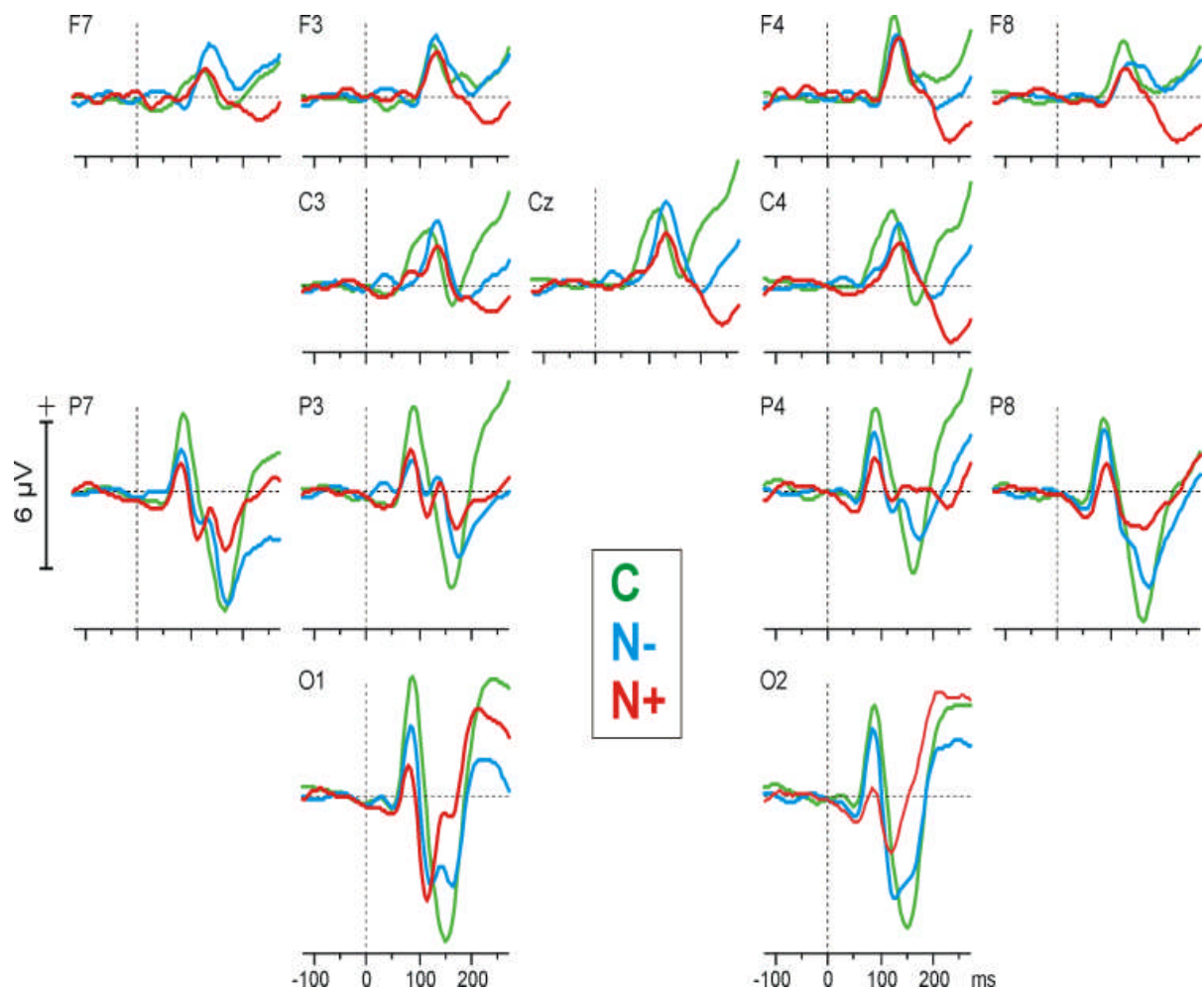
**Suppl. Fig. 2.** Grand average visual event-related potentials (ERPs) for target and non-target stimulus types pooled together in controls (C), patients without neglect (N-), and patients with neglect (N+). Stimulus onset is at 0 ms. Horizontal lines present the baseline.

Time-domain analysis of event-related potentials (ERPs). EEG epochs used for analysis in the time-frequency domain were used for analysis in the time domain. Individual single sweeps of correct responses were averaged against a baseline of 200 ms before stimulus for each electrode and stimulus type.

In the first 200 ms after stimulus, average visual ERPs were characterized by P1 and N1 components **(Fig. S2)**. In both healthy controls and patients (N- and N+) N1 component was composed of two sub-components, an early one within 110-140 ms and a late one within 140-180 ms after stimulus. Peak P1 amplitude and latency and peak N1 latency were measured. Additionally, N1 amplitude was measured as a mean value within 110-140 ms (early N1) and 140-180 ms (late N1).

ERP parameters were subjected to a repeated measures analysis of variance (ANOVA) with one between-subjects variable Group with three levels (control vs. N- vs. N+), and within-subjects variables Stimulus (target vs. non-target), Laterality (left vs. right) and Electrode (ventral parietal – P7/P8, dorsal parietal – P3/P4, and occipital – O1/O2). When significant interactions were yielded, simple effects of within- and between-subjects variables were tested. In case of significant Laterality x Electrode interactions with Group, simple Group effects were explored using MANOVA. Nonsphericity between levels of repeated measures

3

factors in the ANOVAs reported below was corrected using the Greenhouse-Geisser procedure (Greenhouse and Geisser, 1959). Original *df* and corrected *p* values are reported. Significant main and interactive Group effects are described.

RESULTS

*P1 ERP component:* No significant main effects of Group were yielded for P1 amplitude ($F_{(2/30)} = 1.2$, $p = 0.15$) and latency ($F_{(2/30)} = 0.09$, $p = 0.9$), nor were the interactions of Group with Stimulus and topography factors significant ($F_{(4/60)} < 2.3$, $p > 0.1$).

*N1 ERP component:* The amplitude of the early N1 sub-component was not modulated significantly by pathology ($F_{(2/30)} = 0.7$, $p > 0.4$) at any electrode (interactions Group with topography factors, $F_{(4/60)} < 1.6$, $p > 0.1$). As demonstrated in **Fig. S2**, the late N1 sub-component was reduced in neglect patients, being almost absent at right dorsal parietal and occipital electrodes (Laterality x Electrode x Group, $F_{(4/60)} = 3.2$, $p = 0.03$; Simple Group effects at O2, $F_{(2/32)} > 4.2$, $p < 0.05$). Following this ERP morphology effect, N1 peak latency was significantly shorter at occipital sites in neglect patients (mean 115 ms, SE ± 6.9 ms vs. 148 ms, SE ± 6.5 in Control and N- groups). This was reflected by the significant interaction Electrode x Group ($F_{(4/60)} = 3.9$, $p = 0.009$; Simple Group effects at O1 and O2, $F_{(2/32)} > 4.2$, $p < 0.05$).

Reference
1. Greenhouse, S.W., Geisser, S. (1959) On methods in the analysis of profile data. Psychometrika, 24 (2), 95-112.

**Supplementary Material 4 (S4)**

**Control Analyses**

1. Control analysis measures
Following the PLV observations, all control analyses were performed for the relevant frequency ranges, beta and theta.

1.1 Phase-lag index (PLI): To obtain reliable estimates of phase synchronization that are invariant against possible presence of common sources (volume conduction and active reference electrodes), we additionally calculated the phase-lag index (Stam et al., 2007) according to the equation:

$$PLI = \left| \langle sign[\Delta\rho(t_k)] \rangle \right|,$$

where *PLI* denotes the phase-lag index obtained from time series of phase differences $\Delta\rho(t_k)$, $k = 1 \dots N$. PLI ranges between 0 (no coupling or coupling a with phase difference centered around 0 mod $\pi$) and 1 (perfect phase-locking at $\Delta\rho$ different from 0 mod $\pi$), and is in fact an index of the asymmetry of the phase difference distribution (Cohen, 2015).

1.2 Total Power of time-frequency (TF) components: To measure the total activity (total power) comprising the phase-locked and non-phase-locked fractions of TF ERP components, for each trial, the time-varying power in a given frequency band was calculated by squaring the absolute value of the convolution of the signal with the complex wavelet. TF powers were extracted in the relevant (beta and theta) frequency

4

ranges. Maximal TF power and corresponding peak power latencies were measured within 250 ms before and 250 (350) ms after the stimulus for beta (theta). The mean of the pre-stimulus baseline epoch was subtracted from TF power measures at each time point of the analysis epoch for each frequency band and electrode. For statistical evaluation, TF power was log10 transformed.

1.3 Phase-locking factor (PLF): Wavelet transformed single ERP trials were further analyzed to assess the local phase-locking (inter-trial synchronization) of beta and theta TF components by computing the PLF (Lachaux et al., 1999; Tallon- Baudry et al., 1997). The PLF provides a measure of local synchronization of oscillatory activity independently of signal amplitude. The values of PLF yield a number between 0 and 1 determining the degree of phase-locking, where 1 indicates perfect phase alignment across trials and values close to 0 reflect high phase variability. PLF was measured as the mean value of the signal in the post-stimulus time windows used for beta and theta bands according to the 250 ms pre-stimulus baseline.

## 2. Results

### 2.1. Phase-lag index (PLI)

PLI values were analyzed with the ANOVA design used for PLV to check for the replication of major effects. Beta PLI analysis only partially confirmed PLV findings. Beta PLI was reduced in the N+ group for pairs linked by right frontal electrodes (Lat-F x Group, $F(2/31) = 3.4$, $p = 0.05$) and the right parietal electrode P8 (Lat-P x DV-P x Group, $F(2/31) = 6.2$, $p = 0.006$; Lat-P x DV-P effect in N+, $F(1/8) = 6.1$, $p = 0.04$). The complex interaction Lat-F x DV-F x Lat-P x DV-P x Group emphasizing the specific right parietal-left frontal phase relationships in N+ patients was not significant, although the enhancement of synchronization between these regions in N- patients was confirmed for nontargets (Stimulus x DV-F x Lat-P x Group, $F(2/31) = 3.2$, $p = 0.05$).

Theta PLI analysis confirmed major PLV results. Although the synchronization dominated by ventral parietal electrodes P7 and P8 did not reach statistical significance, the between group differences were confirmed for regional frontal synchronization, which was stronger for pairs grouped by dorsal frontal electrodes F3/F4 relative to F7/P7 only in controls, with just opposite (dorsal < ventral) relations in patients (DV-F x Group, $F(2/31) = 7.9$, $p = 0.002$). This distinction was not pronounced at the right hemisphere in neglect patients (Lat-F x DV-F x Group, $F(2/31) = 3.4$, $p = 0.05$). Also, as found for theta PLV, regional parietal synchronization in control and patient groups depended differentially on stimulus processing (Stimulus x Lat-P x DV-P x Group, $F(2/31) = 3.4$, $p = 0.05$). Between-group MANOVA comparisons at F3-P3 and F4-P4 pairs did not reach significance ($p < 0.1$), but interactive effects in each group confirmed that in patients without neglect, synchronization was reduced for pairs grouped by the left dorsal parietal region P3, whereas it was enhanced for right parietal (P8) and frontal (F4) pairs (DV-F, $F(1/10) = 11.9$, $p = 0.006$; DV-F x Lat-P, $F(1/10) = 4.8$, $p = 0.05$; Lat-F x Lat-P, $F(1/10) = 4.9$, $p = 0.05$). Likewise, in patients with neglect, there was an overall reduction of theta PLI for non-targets and a target-related enhancement for pairs grouped by ventral parietal P7 and P8 and left frontal regions (DV-F x Lat-P x DV-P, $F(1/8) = 4.5$, $p = 0.05$; Stimulus x Lat-P x DV-P, $F(1/8) = 5.0$, $p = 0.05$; Stimulus x Lat-F x DV-F x Lat-P x DV-P, $F(1/8) = 13.1$, $p = 0.007$).

### 2.2. Inter-trial synchronization (PLF)

To control for the contribution of local regional synchronization to PLV effects, regional distribution of PLF was evaluated and compared between groups. PLF at four frontal and four parietal electrodes was submitted to a Group x Region (frontal vs. parietal) x Laterality (left vs. right) x DV (dorsal vs. ventral) repeated-measures ANOVA. Local beta synchronization was significantly stronger over parietal than frontal regions (Region, $F(1/31) = 59.9$, $p < 0.001$), but did not manifest hemispheric asymmetry ($p > 0.5$ for Laterality and DV variables). Beta PLF did not depend on pathology at any region (Group, $F(2/31) = 0.4$, $p > 0.6$; Region x Group, $F(2/31) = 0.1$, $p > 9.9$), and only tended to be reduced at right parietal electrodes in patients with neglect (Region x Laterality x Group, $F(2/31) = 3.0$, $p = 0.07$). Accordingly, between-group differences at specific electrodes were not significant as indicated by MANOVAs ($p>0.09$).

Similar to beta, local theta synchronization was significantly stronger at parietal than frontal regions (Region, $F(1/31) = 19.4$, $p < 0.001$) but this effect only stemmed from controls, as there was a substantial reduction of local theta synchronization at parietal locations in patient groups (Region x Group, $F(2/31) = 5.5$, $p = 0.009$; Region effect in controls, $F(1/13) = 28.2$, $p < 0.001$; Region effect in patients, $F < 3.0$, $p > 0.1$). Specifically, the two patient groups manifested reduced local synchronization relative to controls at all parietal electrodes except P8, where PLF was decreased only in patients with neglect (Region x Laterality x DV x Group, $F(2/31) = 3.7$, $p = 0.03$). There was no significant difference between N- and N+ groups at any parietal electrode ($p > 0.1$). Also, only in patients with neglect, PLF was larger to targets than non-targets at right frontal electrodes, whereas the target vs. non-target difference was expressed at parietal locations for other groups (Stimulus x Region x Laterality x Group, $F(2/31) = 4.9$, $p = 0.02$). These observations were confirmed by MANOVA indicating a significant difference between patients and controls at parietal electrodes ($p < 0.05$).

These PLF results demonstrate that local stimulus-related beta synchronization was not affected by pathology, whereas local theta synchronization was substantially reduced at all parietal electrodes in the two patient groups, with no difference between patients without and with neglect.
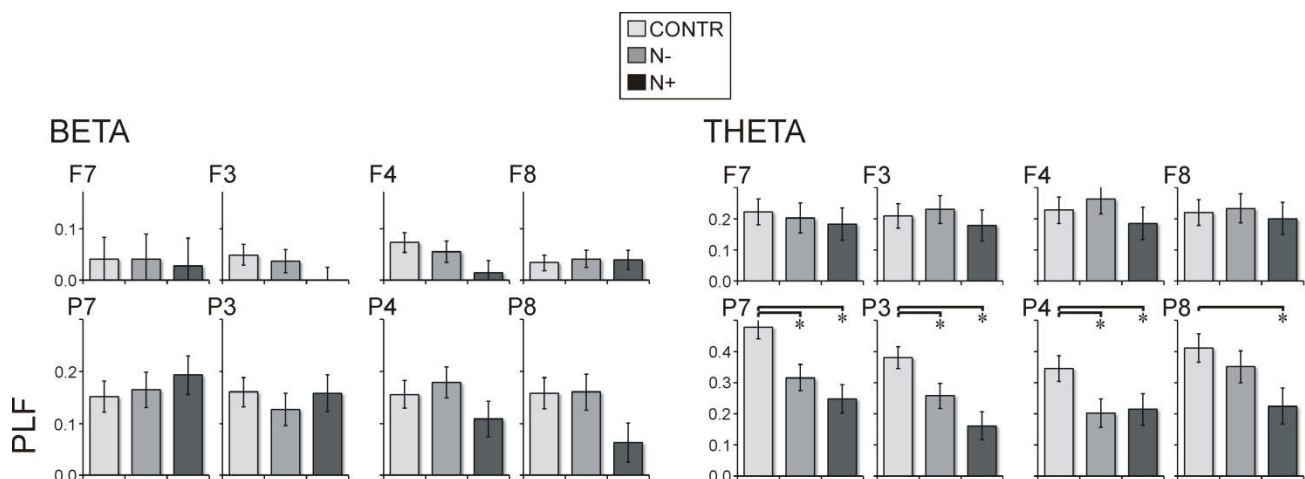


**Suppl. Fig. 3.** Phase-locking factor (PLF) for beta and theta frequency ranges in the three groups (group mean values ± standard errors are presented). The respective frontal and parietal electrodes are designated above each graph. *, $p < = 0.05$.

2.3. The effect of local synchronization on PLV

To further evaluate possible effects of independent stimulus-induced synchronization at multiple regions on PLV, first we tested if PLVs grouped by single electrodes would differ. We used PLV measures in controls and applied paired sample t-tests to compare the four pairs guided by each parietal electrode P7, P3, P4 and P8, where the local inter-trial synchronization was maximal. If PLV were essentially determined by local stimulus-related synchronizations, no difference would exist between pairs guided by the same electrode. For each electrode, significant theta PLV differences existed between 50-100% of the comparisons ($p = 0.001$-$0.05$, Bonferroni corrected $p < 0.005$ for more than 50% of the comparisons), irrespective of whether the local synchronization was large (as for ventral P7 electrode) or weak (as for P4; Lead effect on PLF in controls, $F(3/39) = 4.6$, $p = 0.01$). Beta PLV differences tended to exist between 10-30% of the pairs ($p = 0.02 – 0.05$). These observations demonstrate that local stimulus-induced synchronization might not be a critical determinant of PLV.

In a second analysis with participants from all groups included, the correlations between PLV, PLI, PLF and total power were explored. PLVs grouped by a single electrode were averaged to reflect PLV synchronization guided by that specific electrode. Similarly, PLIs guided by each specific electrode were averaged. Eight multiple step-wise regression analyses were performed for each electrode where PLV was the dependent variable, and PLI, PLF, and total power at that electrode were the predictors. For example, it was tested if PLVs grouped by P7 were predicted by PLIs grouped by P7, PLF at P7, and total power at P7. Significance level was corrected to $p = 0.006$ to control for multiple comparisons. For all analyses of theta PLV, theta PLI was selected as a significant predictor ($F(1/33) = 25.7 – 93.6$, $p < 0.001$; B = $0.85 – 4.4$; Beta = $0.7 – 0.9$). PLI prediction was weaker for beta PLV as PLI was selected as an independent predictor of PLV in half of the models at parietal electrodes. These control observations indicate that PLV measures are basically predicted by PLI measures, which are free of volume conduction and stimulus-induced phase-locking effects, and therefore appear to reflect essential inter-regional connectivity as captured by PLI.

2.4.  Total Power

*Total beta power*: The main Group effect was not significant $F(2/31) = 0.82$, $p > 0.4$). Interactive effects of Group with topography factors were not significant ($F(2/31) < 0.7$, $p > 0.5$). Main and interactive effects of Stimulus were not significant ($F(1/31) < 0.2$, $p > 0.7$). The only significant result reflected an increase in beta power at right dorsal frontal electrode F4 (FP x Laterality, $F(1/31) = 6.3$, $p = 0.02$), which persisted across groups (Group x FP x Laterality, $F(2/31) = 0.83$, $p > 0.4$).
*Total theta power*: The ANOVA design included one between-subjects factor, Group, with 3 levels (controls vs. N- vs. N+),  three within-subjects electrode factors, Frontal/Parietal (FP, frontal vs. parietal), Laterality (left vs. right), and Ventral/Dorsal (VD, ventral vs. dorsal), and Stimulus as an additional within-subjects factor. The main Group effect was not significant ($F(2/31) = 0.9$, $p > 0.4$), nor were interactions with regional and stimulus variables ($p > 0.5$). Theta power was significantly larger for targets than non-targets (Stimulus $F(1/31) = 12.26$, $p = 0.001$). Target-related theta increase was focused to parietal regions (Stimulus x FP ($F(1/31) = 8.1$, $p = 0.008$). Theta power was overall larger over parietal than frontal regions (FP, $F(1/31) = 10.16$, $p = 0.003$).

Peak Latency of Total Power
*Peak beta latency*: Mean peak latency was 104 ms (SE = ±5.1). None of the between- or within-subjects factors was significant for beta latency ($p > 0.3$) except for the interaction of (Group x Stimulus x Laterality, $F(2/31) = 3.9$, $p = 0.03$): In contrast to controls who had longer beta latency over the left than the right hemisphere for the two stimulus types, the

opposite (longer beta latency over the right than the left hemisphere) was observed in neglect patients for non-targets.

*Peak theta latency*: Theta power was maximal around 175 ms (SE = ±7.5 ms). Groups did not differ (F(2/31) = 1.1, p > 0.3). Peak latency was longer at frontal than parietal locations, mean 188±6.7 ms vs. 162±7.1 ms (F(1/31) = 9.34, p = 0.005), which did not depend on pathology (Group x FP, F(2/31) = 0.36, p = 0.7). Theta latency was longer over the right (mean 186±7.6 ms) than the left (mean 163±7.6 ms) hemisphere (Laterality, F(1/31) = 10.6, p = 0.003), but this effect was not observed for non-targets in patients without neglect who manifested decreased latencies over the two hemispheres during non-target processing (Stimulus x Laterality x Group, F(2/31) = 4.5, p = 0.02).

2.5. Correlations between power measures

To further exclude a volume conduction effect on PLV, correlations were examined between total power measures at frontal and parietal electrodes. In case of inter-regional synchronizations induced by a common source or volume conduction, strong positive correlations are expected (Cohen, 2014, 2015). But most of these correlations were negative (r = - 0.2/ -0.004) and those which were positive did not reach significance. Especially pairs with strongest synchronization yielded negative correlations of power at the respective electrodes. Second, the temporal dynamics of power and PLV was different as reflected by latencies of their maximal expression (Suppl. 3). Third, total power at frontal and parietal electrodes did not show the functional reactivity to pathology and stimulus relevance manifested by PLV: Specifically, interactions between Group and topography factors were not significant for total power (p > 0.3). Also, effects of targets vs. non-targets on total power were not consistent with those found for PLV across groups (Suppl. 3). These post-hoc tests show that PLV measures used here may not be produced by common sources.

2.6. PLV of equidistant pairs

An additional argument comes from comparisons of our intra-hemispheric PLVs with PLV of equidistant inter-hemispheric pairs (F3-F4, P3-P4; Philips et al., 2012). Both for theta and for beta, PLV of equidistant trans-hemispheric pairs was smaller (theta: F(3/93) > 35.5, p < 0.0001; beta: F(3/93) > 8.2, p < 0.01).